Engineering Science and Technology, an International Journal 19 (2016) 395–420

HOSTED BY

Contents lists available at ScienceDirect

Engineering Science and Technology, an International Journal

journal homepage: http://www.elsevier.com/locate/jestch

Full Length Article

A novel quasi-oppositional harmony search algorithm for AGC optimization of three-area multi-unit power system after deregulation

Chandan Kumar Shiva, V. Mukherjee *

Department of Electrical Engineering, Indian School of Mines, Dhanbad, Jharkhand, India

ARTICLE INFO

Article history:
Received 25 April 2015
Received in revised form
9 July 2015
Accepted 30 July 2015
Available online 18 September 2015

Keywords:
Automatic generation control
Bilateral contracts
Deregulation
Optimization
Quasi-opposite number

ABSTRACT

The present work addresses a decentralized, well tested three-area multi-unit power system for its automatic generation control (AGC) after deregulation which is characterized by price-based market operation. To match with the actual deregulated environment, as prevailing in the real one, the market structure is kept generic enough enabling to capture all possibilities occurring in real-time day-to-day power environment. In accordance to the modifications, as done in the investigated three-area power system model, the concerned objective is to intensify the deregulated AGC operation followed by load disturbances. At the present platform, three different classes of case study results are postulated for the studied test system. The first two illustrate the behavior of unilateral and bilateral based power contract transactions while the third one considers the contract violation case as it exists in present time. The contractual agreement, instituted by DISCO participation matrix, is initialized to address the power transaction contracts. In this work, a novel quasi-oppositional harmony search (QOHS) algorithm is explored and presented its significances in deregulated AGC operation. In the second phase of investigation, fast acting Sugeno fuzzy logic technique is explored for on-line, off-nominal operating conditions. For analysis purpose, both the qualitative and the quantitative aspects of the proposed QOHS are presented in reference to genetic algorithm (GA). Additionally, the sensitivity analysis is also performed to evaluate the performance of the proposed QOHS based controller. Simulation work reveals that the proposed QOHS may be, effectively, worked out to order to improve the deregulated AGC performance. It is also being observed that the proposed QOHS outperforms the GA in sense of deregulated AGC operation of power system.

1. Introduction

1.1. General

At present, the electric power industry is, largely, in the control of vertically integrated utilities (VIUs) which have their own generation–transmission–distribution systems. It supplies powers to the customers as per automatic generation control (AGC) criteria. One VIU is, usually, interconnected to other VIUs and this interconnection is always at the transmission voltage level [1]. When concerning AGC control strategy, the conventional *tie-line bias control* concept is adopted where a single utility company has its own one control area and, hence, may locate the control error according to its own desire [2]. After the huge success of AGC in VIUs, the concept of price-based market operation is the missing index that has changed the entire structure of the power industry. In view of this, a new deregulated power system has evolved, although keeping all essential ideas the same as per AGC. The purpose is to orient a price-based operation, supervised by AGC and classified by the new market structure.

In essence, deregulation is collective sums of market policies, economic benefits as well as good qualities of services that may be used for the optimum benefits of the customers. Functionally, the process of deregulation starts with the emergence of independent generation companies (GENCOs), distribution companies (DISCOs), transmission companies and independent service operator (ISO) [3]. These independent entities have to play distinct roles in AGC domain and, therefore, have to model differently.

In deregulated AGC system, load following may be the most important aspect of observation. Corresponding to this, the deviation in frequencies and the tie-line power flow profiles might be the mysterious questions of a priori importance. At the instant application of load demands, the most influenced state (affected part) is the actual generated powers of the GENCOs. The GENCOs generated

* Corresponding author. Tel.: +91 0326 2235644; fax: +91 0326 2296563.
E-mail address: vivek_agamani@yahoo.com (V. Mukherjee).
Peer review under responsibility of Karabuk University.

http://dx.doi.org/10.1016/j.jestch.2015.07.013

profiles, at the steady state of each control area, must reach their desired values according to their participation factors as decided for the DISCOs load demands.

In this new challenging paradigm, AGC must have a deep sense of responsibly to overcome the contractual effects as made concerning quality services [4]. The root of success of deregulation lies in the fact that a DISCO has the complete freedom to contract, individually, with any GENCO in its own control area and/or to other areas for the transaction of powers which is supervised by the ISO. The path of these power transactions is followed by the DISCO participation matrix (DPM) [5].

1.2. Literature review

Interconnected power system modelling, its control strategies and operational behavior play important roles in deregulated power system operation and control. Over the last few decades, significant amounts of in depth discussions have been attributed in connection to interconnected power systems (viz. VIUs) regarding AGC performance study. A major portion/contribution of these research works are addressed in References 4 and 6.

The crucial role of AGC is continuing in the domain of deregulated power system oriented by price-based operation and accounting various bilateral policies. In view of this, the necessary modifications as required in the conventional AGC system to study the load following deregulated operation have been reported in References 4 and 7. In these two works, the difference between the AGC operation in VIUs (conventional paradigm) and the horizontally integrated industry (new paradigm) has been highlighted. Also, the deregulated AGC model, its control strategies and various deregulated cases have been unveiled.

The recently reported works on deregulated AGC domain reveal that significant numbers of optimization techniques have been used, classified by different theories (*i.e.* mathematical computational techniques, optimal control concepts, evolutionary optimization algorithms etc.) to enhance the AGC performance of deregulated power system. AGC optimization using mathematical computational techniques have been reported in References 8 and 9. In these two research works, an iterative procedure in view of finding the proportional-integral-derivative (PID) controller gains has been introduced. Also, the analytical expressions have been derived for finding the boundaries of equality constraints set on proportional-integral (PI) gains. The formulation and the solution of multi-objective AGC problem in deregulated environment using the mixed H_2/H_∞ control approach have been reported in Reference 10. A deregulated AGC model, oriented by multi-stage fuzzy-PID controller, has been suggested in Reference 11. The impacts of internal model control method in deregulated AGC domain have been studied by Tan et al. [12]. Likewise, the significance of linear active disturbance rejection control method has been investigated for load frequency control (LFC) issue after deregulation in Reference 13. The assessment of dynamic reliability for bilateral contract of electricity providers has been presented by Ding et al. [14]. AGC simulation of deregulated multi-area power system has been carried out by Bhatt et al. [15] using hybrid particle swarm optimization (PSO) algorithm. Likewise, the performance of a fractional-order PID controller in deregulated power market has been evaluated in Reference 16 by using the bacteria foraging optimization algorithm (BFOA).

1.3. Motivations behind the present work

Literature survey divulges that a number of AGC techniques have been proposed in deregulated power system. These techniques have, significantly, contributed in the initial development of deregulated AGC operation. But, at the same time, no sophisticated methods have been proposed in AGC formulation due to some inherent drawbacks as prevailing in the adopted techniques.

The good choices of initial condition and the selection of derivative gain play crucial roles in the iterative method that affect the AGC performance [9,17]. The fuzzy-PI controller does not produce satisfactory dynamic responses. However, the fuzzy-PID controller produces somewhat better AGC results but, at the same time, requires a three-dimensional rule base which is difficult to design [18]. All in one, the intelligence-based PID controller is a once-for-all method, which means that once the optimization is completed, the parameters are hard to re-tune. Control system based tuning methods need to use full states of a control area (as the feedback input signal) which is, in reality, a difficult task as some of them lead to high-order controllers while the others are too complex to be understood [13,19].

Reflecting to optimization techniques, both the binary coded genetic algorithm (GA) and the real coded GA has received considerable attention as optimization tool by the researchers' pool for several engineering applications. However, these two techniques are susceptible to the choice of mutation probability and crossover ratio. The generated solutions may stick to suboptimal solutions [15]. PSO is developed through the simulation of bird flocking in multi-dimensional search spaces. Empirical studies, performed on PSO, indicate that even when the maximum velocity and acceleration constants are correctly defined, the particles may still diverge *i.e.*, go to infinity (a phenomena known as "*explosion*" of the swarm). BFOA is based on chemotactic movement of virtual bacterium models *i.e.* instituted by trial solutions of the optimization problem. During the process of chemotaxis, the performance of BFOA depends on random search direction that may lead to delay in reaching the global solutions. Also, the number of parameters, as used in BFOA for searching the total solution space, is higher than GA and, hence, the possibility of trapping into local minima is higher than GA.

The problem of concern is that optimized controller gains as obtained so far by the application of various optimization techniques are not close to their global optimal solutions. These controller gains exhibit unsatisfactory dynamic responses and, directly, affect the AGC performance. It may also be inferred that the earlier adopted methods are not convenient in deregulated AGC system owing to their own problems and limitations. Moreover, recently developed optimization techniques have not been used in deregulated AGC domain that may satisfy the multi-objective AGC problems (such as stability, robustness, optimal performance etc.) up to a satisfactory level.

To overcome the above mentioned difficulties, a new evolutionary population based searching technique is proposed. In this paper, an approach (harmony search (HS) algorithm (HSA)) based on musical improvisation process is presented in order to solve AGC problem. HSA is a derivative-free real parameter optimization algorithm and may be used in various fields of engineering applications [20,21]. Along with HSA, a few modified variants of HSA have been also proposed for enhancing its solution accuracy and convergence profile speed. Mahdavi et al. [22] have presented an improved HSA by introducing an idea of constant parameters so as to, dynamically, tune its key parameters. Omran and Mahdavi [23] have proposed a global best HSA by utilizing the concept of swarm intelligence. Pan et al. [24] have proposed a self-adaptive global best HSA for solving continuous optimization problems. Banerjee et al. [25] have proposed oppositional-based HSA for reactive power compensation of an autonomous power system model.

The behavior of a synchronous generator in connection to AGC of power system depends on many factors. These are: (a) its position in the network, (b) the operating conditions, (c) the network topology and (d) the generation schedule. Usage of a desired optimization technique yields a distinct set of controller gains for different operating conditions. Under drastic change in operating

condition, the nominal controller is not necessarily going to be tuned enough to yield satisfactory performance. For on-line tuning of the PID controller gains, very fast acting Sugeno Fuzzy Logic (SFL) technique is adopted. A SFL based controller adjusts its parameters online according to the environment in which it works. The specialty of SFL lies within the fact that it provides good dynamic responses over a wide range of variation in system parameters [26]. Off-line conditions are sets of nominal system operating conditions. The work of SFL is to extrapolate the nominal optimal PID gains, intelligently and linearly, in order to determine off-nominal optimal controller gains. In real-time environment, these input conditions may vary, dynamically, and become off-nominal ones. This necessitates the use of very fast acting SFL in order to determine the off-nominal controller parameters for off-nominal input operating conditions. The SFL technique has many advantages such as efficiency in computation and no requirement of extra time in the defuzzification process.

The present work explores the significance of HSA as an optimization tool for its utilization in a deregulated power system. This work is further extended in view of AGC optimization problem concerning the design of controller gains installed in each area of the power system. The analytical behaviors of HSA in the field of optimization that enforces to use in the present work are that it [27]:

(a) uses stochastic random search rather than gradient search and, thus, any derivative information is unnecessary,
(b) generates a new solution vector after considering all the entire solution vectors,
(c) needs fewer mathematical calculations,
(d) identifies the high performance region of the solution spaces,
(e) has the potential ability to converge to quality solutions and
(f) avoids trapping into local minima due to its unique dispersal and elimination qualities.

In the present optimization task, a modified variant of HSA is applied as a solution to the reported problems and limitations. The present work utilizes the quasi-oppositional concept in the basic HSA and, thus, the new variant of HSA is named as quasi-oppositional HS (QOHS) algorithm. The proposed QOHS houses both the characters of two guesses (*i.e.* opposite-point and quasi-opposite point) to enhance the performance region of the solution space(s). Thus, in turn, it may offer the potential ability to convergence rapidly near the optimal solution regions [27]. The entire work focuses on the impacts of the proposed QOHS for power system application in the domain of deregulated AGC subject.

1.4. Contributions of the present work

The main contributions are to:

(a) design an AGC model of three-area multi-unit deregulated power system,
(b) present a systematic view of a novel QOHS algorithm as an optimization tool,
(c) test the proposed QOHS on a set of five benchmark functions in order to validate the performance of the algorithm,
(d) execute the proposed QOHS in the AGC simulation of the studied test system for the computation of optimal PID controller gains,
(e) explore the feasibility of SFL in real-time deregulated environment,
(f) compare the suitability of the studied GA-SFL and the proposed QOHS-SFL in deregulated AGC performance and
(g) discuss the sensitivity and computational cost scenarios for the proposed QOHS.

1.5. Organization of the present paper

The layout of the rest of the paper is documented in the following sequences. Various aspects of deregulated scenarios are explained in Section 2. Details of the studied deregulated three-area power system model are introduced in Section 3. In Section 4, the formulation of the objective function and its physical constraints are presented. A brief description of the proposed QOHS is rendered in Section 5. Section 6 introduces the basic concept of GA. Section 7 investigates the SFL in deregulated AGC operation. Simulation results, their discussions, sensitivity and computational cost analysis are presented in Section 8. Finally, the concluding remarks are presented in Section 9.

2. Aspects of deregulated AGC study

Deregulated power system is being instituted by various power transactions such as unilateral, bilateral based and the contract violation case. These power transactions have to follow the AGC criteria. Thus, the desired objectives of AGC are to maintain the (a) system frequency at or very close to the specified nominal range, (b) power flow in the interlinking tie-lines among the areas closer to their scheduled values and (c) generation of each unit at their most economical proportion [15].

In case of unilateral transaction, GENCOs participate in AGC of their own areas only [8]. In bilateral based one, a GENCO of any area may supply power to DISCOs in its user pool as well as DISCOs in other areas through the tie-lines and submitted their contractual agreements to the ISO. In such agreements, GENCOs send pulses to the governor to follow the predicted loads as long as these do not exceed the contracted value. In the same framework, the responsibilities of the DISCOs are to monitor their loads continuously and to ensure that the loads following requirements are met in accordance to the contractual agreements made [3]. For the flexibility of open market, both the unilateral and the bilateral based transactions operate, simultaneously, *i.e.* a DISCO and a GENCO of any control area may negotiate for bilateral contract. In such contracts, GENCOs may change their output power supply as long as these do not exceed the contracted load.

The facility of any DISCO to buy power at a competitive price from other GENCOs which may or may not have contracted in the same area, a matrix termed as DPM, is initialized [5]. Essentially, DPM provides the overall participation of a DISCO in contract with all GENCOs. The configuration of DPM suggests that the number of rows and the columns are equal to the number of GENCOs and the DISCOs, respectively. Each element of DPM is configured as contract participation factor (cpf_{ij}) which specifies the fraction of total load power contracted by the jth DISCO from the ith GENCO. As a result, a total sum of entries of a column belonging to each DISCO is unity. Mathematically, it is expressed as $\sum_i cpf_{ij} = 1$.

In case of more than one GENCO in a particular area, *ACE* signal must be shared in proportion to their *ACE* participation factor (*apf*). Mathematically, the individual contribution of each GENCO of ith control area may be stated by equation (1).

$$\sum_{j=1}^{n_i} apf_{ji} = 1 \tag{1}$$

The expression for total load demand (ΔP_{total}) of each ith control area may be stated by equation (2)

$$\Delta P_{total} = \Delta P_{loc,i} + \Delta P_{di} \tag{2}$$

where $\Delta P_{loc,i} = \sum_{j=1}^{m_i} \Delta P_{L\,ji}$ is the total local contracted demand whereas $\Delta P_{di} = \sum_{j=1}^{m_i} \Delta P_{UL\,ji}$ refers to total un-contracted demand.

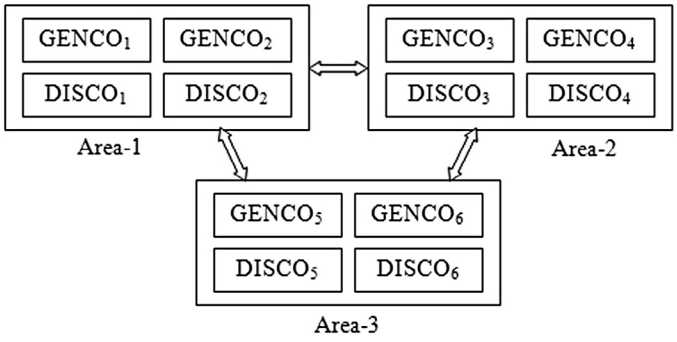

Fig. 1. Layout view of the deregulated three-area multi-unit test power system [30].

The generalized expression for generated powers of each GENCO ($\Delta P_{m,ki}$) may be stated by equation (3)

$$\Delta P_{m,ki} = \rho_{ki} + apf_{ki}\sum_{j=1}^{m_i}\Delta P_{UL\ ji} \quad k = 1, 2, \ldots, n_i \tag{3}$$

where ρ_{ki} is the contracted load demand of $GENCO_{ki}$ which may be expressed by equation (4).

$$\rho_{ki} = \sum_{j=1}^{N}\sum_{t=1}^{m_j} cpf_{(si+k)(sj+t)}\Delta P_{L\,tj} \tag{4}$$

3. Deregulated AGC power system model

3.1. Structure of PID controller

In AGC performance, the role of PID is to supervise the LFC mechanism by minimizing the area control error (ACE) owing to deviation in rated load. Also, it ensures the dynamic stability of the plant model. The execution of PID to a plant model increases the type of the system and, as an effect of this, the steady state error will be zero for the application of step load demand. The PID calculates the average error of the plant model and, in that respect, it generates controlled output to minimize the plant error. It should be kept in mind that the controller gains must not be too high, otherwise, unstability may result [28].

The control signal ($u(s)$) (*i.e.* amount of control action taken by the controller) may be expressed by equation (5)

$$u(s) = G_{PID}(s) \times ACE \tag{5}$$

where $G_{PID}(s)$ may be stated by equation (6) [29].

$$G_{PID}(s) = K_p + \frac{K_i}{s} + sK_d \tag{6}$$

In equation (6), K_p, K_i and K_d are the proportional, integral and derivative gains of the PID controller, respectively.

3.2. Designing aspects of deregulated three-area power system model

To illustrate the effectiveness of the proposed QOHS, an interconnected deregulated three-area power system model is considered as test system for this work. In view of this, the simplified AGC model is presented in Fig. 1. The complete AGC model, designed in deregulated regime, is endorsed in Fig. 2. The test system is assumed to contain two equal reheat turbine type thermal units in both the areas (*i.e.* area-1 and area-2) while area-3 contains two hydro units [30]. In the present study, the rated power capacity of each *i*th area (ΔP_{ri}) is assumed to be equal (*i.e.* $P_{r1} = P_{r2} = P_{r3}$).

The open loop transfer function (OLTF) for reheat thermal system ($Q(s)$) (for units 1–4) may be stated by equation (7).

$$Q(s) = \left(\frac{1}{(1+sT_g)}\right)\left(\frac{(1+sK_rT_r)}{(1+sT_r)(1+sT_t)}\right)\left(\frac{K_p}{(1+sT_p)}\right) \tag{7}$$

Similarly, the OLTF for hydro-turbine power system ($G(s)$) (for units 5–6) may be stated by (8).

$$G(s) = \left(\frac{1}{1+sT_1}\right)\left(\frac{1+sT_2}{1+sT_3}\right)\left(\frac{1-s}{1+sT_w}\right)\left(\frac{K_{p3}}{1+sT_{p3}}\right) \tag{8}$$

In equation (7), it may be noted that T_g, T_t and T_{ps} are time-constants (in seconds) of governor, reheat turbine and power system dynamics, in order; K_r, T_r and K_{ps} are reheat gain system, reheat time-constant (in seconds) and power system gain constant (in Hz/p.u.MW), respectively, of thermal plant model. As referred to equation (8), T_1, T_2, T_3 are time-constants of hydro governor (in seconds); T_w is water starting time (in seconds); K_{p3} and T_{p3} are the hydro power system gain constant (in Hz/p.u.MW) and time-constant (in seconds), respectively.

To match the generation and the distribution of powers, information signals must flow from the DISCO to the particular GENCOs, specifying corresponding demands. Owing to the presence of six GENCOs and six DISCOs in the studied plant model, there may be a combination of thirty-six *cpf* elements in DPM. These bilateral agreements may be stated by equation (9).

$$\mathrm{DPM} = \begin{bmatrix} cpf_{11} & cpf_{12} & cpf_{13} & cpf_{14} & cpf_{15} & cpf_{16} \\ cpf_{21} & cpf_{22} & cpf_{23} & cpf_{24} & cpf_{25} & cpf_{26} \\ cpf_{31} & cpf_{32} & cpf_{33} & cpf_{34} & cpf_{35} & cpf_{36} \\ cpf_{41} & cpf_{42} & cpf_{43} & cpf_{44} & cpf_{45} & cpf_{46} \\ cpf_{51} & cpf_{52} & cpf_{53} & cpf_{54} & cpf_{55} & cpf_{56} \\ cpf_{61} & cpf_{62} & cpf_{63} & cpf_{64} & cpf_{65} & cpf_{66} \end{bmatrix} \tag{9}$$

As referred to in equation (9), the main diagonal elements refer to demand of each DISCO in its own area only whereas the off-diagonal ones respond to the demands of the DISCOs in one area to the GENCOs in other areas.

The expression for scheduled tie-line power flow ($\Delta P_{tieij(scheduled)}$) may be expressed by equation (10) [31].

$$\Delta P_{tieij(scheduled)} = \left\{\begin{array}{l}(\text{Demand of DISCOs in area} \\ -\ j \text{ from GENCOs in area} - i) \\ -(\text{Demand of DISCOs in area} \\ -\ i \text{ from GENCOs in area} - j)\end{array}\right\} \tag{10}$$

The net deviations of scheduled tie-line power flow (ΔP_i) of each area may be expressed by equations (11) to (13), in order.

$$\Delta P_{1(scheduled)} = \Delta P_{12(scheduled)} + a_{31}\Delta P_{31(scheduled)} \tag{11}$$

$$\Delta P_{2(scheduled)} = \Delta P_{23(scheduled)} + a_{12}\Delta P_{12(scheduled)} \tag{12}$$

$$\Delta P_{3(scheduled)} = \Delta P_{31(scheduled)} + a_{23}\Delta P_{32(scheduled)} \tag{13}$$

The net deviation of power ($\Delta P_{i(error)}$) may be expressed by equation (14).

$$\Delta P_{i(error)} = \Delta P_{i(actual)} - \Delta P_{i(scheduled)} \tag{14}$$

In AGC operation, $\Delta P_{i(error)}$ must vanish as the actual tie-line power deviation ($\Delta P_{i(actual)}$) traps the net scheduled power flow deviation

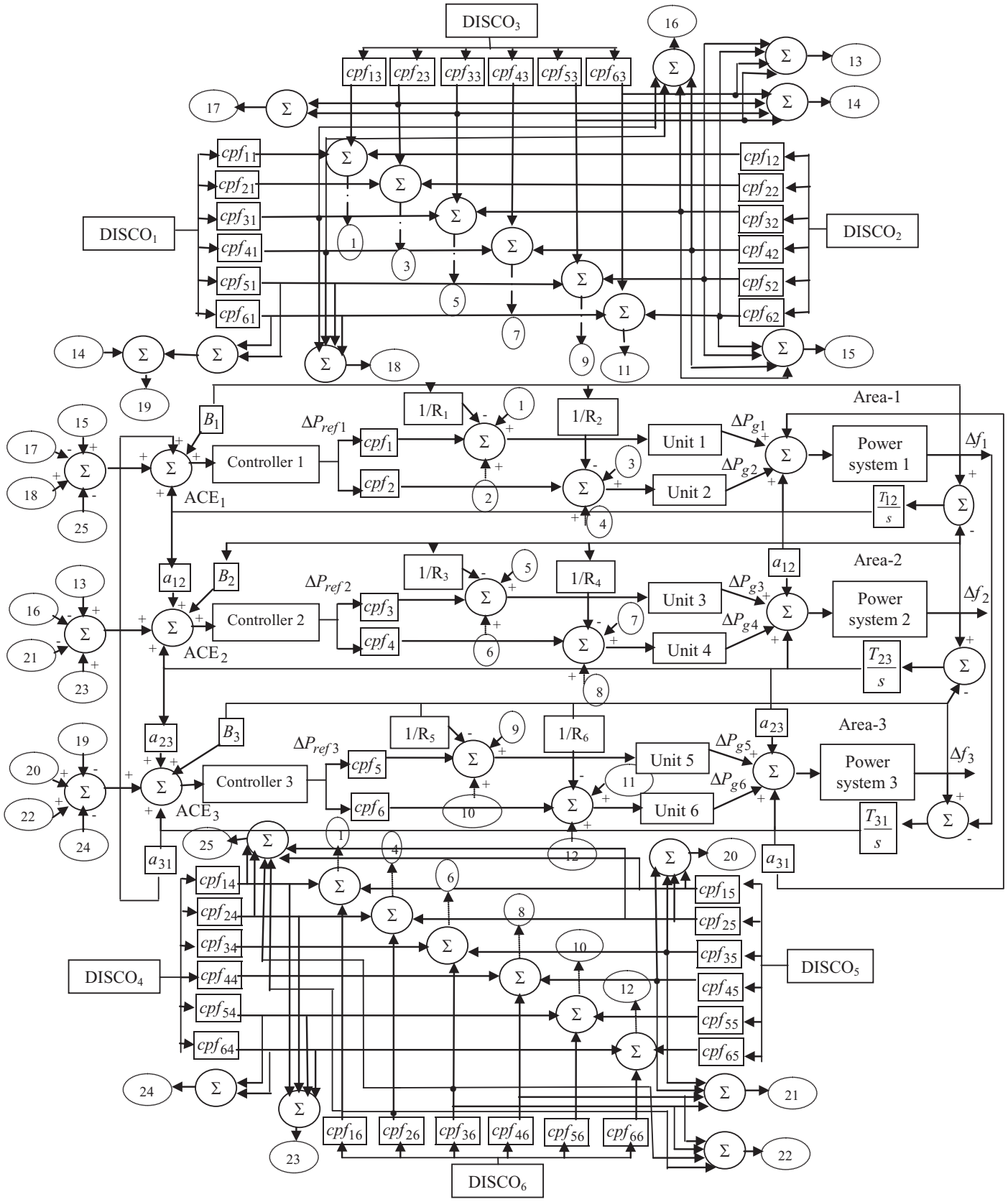

Fig. 2. Configuration of the studied AGC model of three-area power system in deregulated domain [30].

($\Delta P_{i(scheduled)}$) in the steady state. These error signals that contribute to the generation of ACE signal may be stated by equation (15) [5,8]

$$ACE_i = B_i \Delta f_{i(error)} + \Delta P_{i(scheduled)} \quad i = 1, 2, 3 \tag{15}$$

where B_i and Δf_i are the frequency bias coefficient and the frequency deviation of ith area, respectively.

4. AGC problem formulation

4.1. Design of objective function

The present work is designed on the eve of obtaining the optimal PID gains for the optimum performance of the studied deregulated AGC model as presented in Fig. 2. To enhance the system damping characteristics, an objective function is defined and, subsequently, formulated by desired specifications and constraints. To check the worth of a solution vector in the harmony memory, fitness function *i.e.* the integral of square error (ISE) criteria (also termed as figure of demerit (FOD)) may be evaluated by equation (16)

$$FOD = ISE = \int_0^{t_s} \left(\Delta f_i^2 + \Delta P_{tieij}^2\right) dt \tag{16}$$

where t_s is the time range of simulation (in seconds).

The objective of the present study may be stated by equation (17).

$$Min\ FOD = Min\ ISE \tag{17}$$

The purpose of minimization of FOD is to obtain the optimal set of PID controller gains such that the system output responses yield the desired AGC performance of the test system under study. The first term in equation (16) indicates the total frequency deviations of the test system to be constructed. The second term signifies the total deviations in regulated power flow from the rated one. From equation (17), it may be concluded that the lower the FOD value, the better the optimized PID controller gains.

4.2. Constraints of the AGC optimization problem

The constraints of the present optimization task are the gains of the PID controller. The problem constraints are the optimized parameter bounds. Therefore, the design problem may be formulated as an optimization problem framed in equation (18)

$$\left.\begin{aligned} K_{pi}^{\min} \le K_{pi} \le K_{pi}^{\max}, \quad i = 1, 2, 3 \\ K_{ii}^{\min} \le K_{ii} \le K_{ii}^{\max}, \quad i = 1, 2, 3 \\ K_{di}^{\min} \le K_{di} \le K_{di}^{\max}, \quad i = 1, 2, 3 \end{aligned}\right\} \tag{18}$$

where the superscripts *min* and *max* represent the minimum and the maximum values of the respective variables.

The important factor that affects the optimal solutions (more or less) is the range of superscripts, decided by the type of application. Initially, any evolutionary algorithm executes randomly within the high region of the solution spaces. After getting the solutions, one may shorten the solution space nearer to the values, as obtained in the last iteration. Here, the proposed approach employs QOHS in order to solve this optimization problem and search for optimal set of PID controllers' gains (like $K_{pi}, K_{ii}, K_{di}, i = 1, 2, 3$). In this work, the maximum and the minimum ranges of controller gains lie within –0.0010 and –19.9899, respectively.

4.3. Measure of performance

In the present work, an increased amount of emphasis on the mathematical formulation is presented with an aim to improve the design of the system or to design an adaptive system. Regarding this, in addition to the confined objective function defined in equation (16), the three more performance indices (such as integral of time absolute error (ITAE), integral of time square error (ITSE) and integral of absolute error (IAE)) may also be considered for the evaluation of the performance consistency of the proposed QOHS based PID controller design. These three performance indices may be stated by equations (19) to (21), in order.

$$ITAE = \int_0^{t_s} \left(|\Delta f_i| + |\Delta P_{tieij}|\right) t\, dt \quad i = 1, 2, 3 \tag{19}$$

$$ITSE = \int_0^{t_s} \left(\Delta f_i^2 + \Delta P_{tieij}^2\right) t\, dt \quad i = 1, 2, 3 \tag{20}$$

$$IAE = \int_0^{t_s} \left(|\Delta f_i| + |\Delta P_{tieij}|\right) dt \quad i = 1, 2, 3 \tag{21}$$

The values of these three performance indices are calculated at the end of the developed program to access the performance of the designed controller installed in the studied three-area power system model.

5. Formation of QOHS algorithm

5.1. Overview of HSA

HSA is a new derivative-free, real-parameter optimization algorithm, inspired by the improvisation process for searching the perfect state of harmony (solution) [20]. As visualized in HSA, each musician corresponds to each decision variable; a musical instrument's pitch range corresponds to a decision variable's range; musical harmony (at certain time) responds to the solution vector at certain iteration and audience's aesthetics correspond to objective function. As musical harmony is improvised from time to time, solution vector gets improved iteration by iteration cycle [32]. Such an efficient search for a perfect state of harmony is analogous for finding the optimal solutions to various engineering problems. HSA and its variants have been applied to a wide arena of real-life optimization problems such as scheduling of multiple dam system, load dispatch, ecological conservation, industrial operation, musical composition etc.

The optimization procedure of HSA may be sketched below.

Step (a)	*Initialization*: The program parameters are defined and, subsequently, the harmony memory (HM) is initialized with as many random generated solution vectors as the HM size.
Step (b)	*Harmony improvisation*: A new harmony vector is generated based on memory consideration, pitch adjustment and random selection.
Step (c)	*Selection*: When the specified condition is satisfied, the best harmony among the HM is updated. Otherwise, Step (a) and Step (b) are repeated, sequentially.

Based on the work reported by Banerjee et al. [25], the computational procedure of HSA may be presented in Algorithm 1. The notations as used in Algorithm 1 are symbolized in Reference 25. As viewed in Algorithm 1, the HS parameters are harmony memory size (*HMS*), harmony memory consideration rate (*HMCR*), pitch adjusting rate (*PAR*), distance bandwidth (*BW*), number of improvisations (*NI*) and total number of search spaces (*i.e.* dimension of the problem) (*d*).

Algorithm 1: Pseudo code for the HSA [25]

Step 1 Set the parameters: HMS, $HMCR$, PAR, BW, NI and d.

Step 2 Initialize the HM and calculate the objective function value for each harmony vector.

Step 3 Improvise the HM filled with the new harmony X^{new} vectors as follows:

for ($j = 0;\ j < d;\ j++$)

if ($r_1 < HMCR$) then

$x_j^{new} = x_j^a$ % $a \in (1,2,.....,HMS)$

if ($r_2 < PAR$) then

$x_j^{new} = x_j^{new} \pm r_3 \times BW$ % $r_1, r_2, r_3 \in [0,1]$

end if

else

$x_j^{new} = para_j^{\min} + r \times (para_j^{\max} - para_j^{\min})$ % $r \in [0,1]$

end if

end for

Step 4 Update the HM as $X^{worst} = X^{new}$ if $f(X^{new}) < f(X^{worst})$.

Step 5 If NI is completed, return the best harmony vector X^{best} in the HM; otherwise go back to **Step 3.**

The basic HSA uses fixed values for PAR and BW parameters. The improved HSA, proposed by Mahdavi et al. in Reference 33, applies the same memory consideration, pitch adjustment and random selection as in basic HS [34] but updates the values of *PAR* and *BW*, dynamically, may be stated by equations (22) and (23), in order.

$$PAR(gn) = PAR^{\min} + \frac{PAR^{\max} - PAR^{\min}}{NI} \times gn \tag{22}$$

$$BW(gn) = BW^{\max} \times e^{\left(\frac{\ln\left(\frac{BW^{\min}}{BW^{\max}}\right)}{NI} \times gn\right)} \tag{23}$$

In equation (22), $PAR(gn)$ is the pitch adjustment rate in the current generation (gn), $PAR^{\min}$ and $PAR^{\max}$ are the minimum and the maximum adjustment rate, respectively. In equation (23), $BW(gn)$ is the distance bandwidth at generation (gn) whereas $BW^{\min}$ and $BW^{\max}$ are the minimum and the maximum bandwidths, respectively.

5.2. Proposed QOHS algorithm

HSA is improvised by employing the quasi-opposition based learning concept in order to enhance its solution accuracy and accelerate the convergence profile speed. The pseudo code for the proposed QOHS is presented in Algorithm 2. Here, $X_{0i,j}$ is an initial population whereas $OX_{0i,j}$ and $QOX_{0i,j}$ are the mirror images and the quasi-opposite point of $X_{0i,j}$ (for $i = 1, 2, \ldots\ldots\ldots, HMS$ and $j = 1, 2, \ldots\ldots\ldots, d$), respectively [25,35]. The flowchart of the proposed QOHS is sketched in Fig. 3 [35].

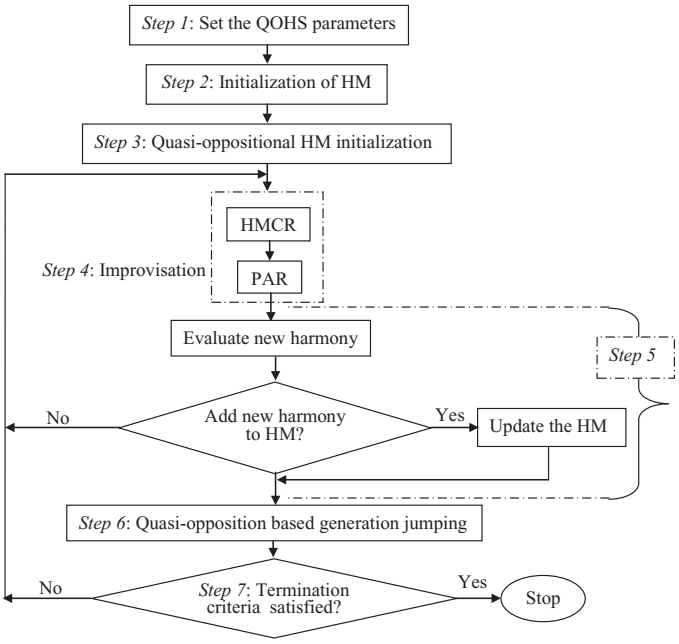

Fig. 3. Flowchart of the proposed QOHS algorithm [35].

Algorithm 2: Pseudo code for the proposed QOHS algorithm

Step 1 Set the parameters: HMS, $HMCR$, $PAR^{\min}$, $PAR^{\max}$, $BW^{\min}$, $BW^{\max}$ and NI.

Step 2 Initialize the HM with $X_{0_{i,j}}$.

Step 3 **% Quasi-oppositional HM initialization**

for ($i = 0;\ i < HMS;\ i++$)

for ($j = 0;\ j < d;\ j++$)

$OX_{0_{i,j}} = para_{i,j}^{\min} + para_{i,j}^{\max} - X_{0_{i,j}}$; % OX_0: Opposite of initial X_0

$M_{i,j} = (para_{i,j}^{\min} + para_{i,j}^{\max})/2$;

if ($OX_{0_{i,j}} < M_{i,j}$)

$QOX_{0_{i,j}} = M_{i,j} + (OX_{0_{i,j}} - M_{i,j}) \times r_1$; % $r_1 \in [0,1]$

end if

else

$QOX_{0_{i,j}} = OX_{0_{i,j}} + (M_{i,j} - OX_{0_{i,j}}) \times r_1$;

end else

end for

end for

% End of quasi-oppositional HM initialization.

Select HMS fittest individuals from set of $\{X_{0_{i,j}}, QOX_{0_{i,j}}\}$ as initial HM; HM being the matrix of fittest X vectors

Step 4 Improvise a new harmony X^{new} as follows:

Update $PAR(gn)$ and $BW(gn)$.

for ($i = 0;\ i < HMS;\ i++$)

for ($j = 0;\ j < d;\ j++$))

if ($r_2 < HMCR$) then

$X_{i,j}^{new} = X_{i,j}^{a}$; % $a \in (1,2,.....,HMS)$

if ($r_3 < PAR(gn)$) then

$X_{i,j}^{new} = X_{i,j}^{new} \pm r_4 \times BW(gn)$; % $r_2, r_3, r_4 \in [0,1]$

end if

else

$X_{i,j}^{new} = para_{i,j}^{\min} + r_5 \times (para_{i,j}^{\max} - para_{i,j}^{\min})$; % $r_5 \in [0,1]$

end else

end if

end for

end for

Step 5 Update the HM as $X^{worst} = X^{new}$ if $f(X^{new}) < f(X^{worst})$

Step 6 **Quasi-opposition based generation jumping**

if ($r_6 < J_r$) % $r_6 \in [0,1]$, J_r: Jumping rate

for ($i = 0;\ i < HMS;\ i++$)

for ($j = 0;\ j < n;\ j++$)

$OX_{i,j} = para_{i,j}^{\min}(gn) + para_{i,j}^{\max}(gn) - X_{i,j}$;

% $para_{i,j}^{\min}(gn)$: minimum value of j^{th} variable of i^{th} parameter in the current generation (gn)

% $para_{i,j}^{\max}(gn)$: maximum value of j^{th} variable of i^{th} parameter in the current generation (gn)

$M_{i,j} = \{para_{i,j}^{\min}(gn) + para_{i,j}^{\max}(gn)\}/2$;

if ($X_{i,j} < M_{i,j}$)

$QOX_{0_{i,j}} = M_{i,j} + (OX_{0_{i,j}} - M_{i,j}) \times r_7$; % $r_7 \in [0,1]$

end if

else

$QOX_{0_{i,j}} = OX_{0_{i,j}} + (M_{i,j} - OX_{0_{i,j}}) \times r_7$;

end else

end for

end for

end if

Select HMS fittest HM from the set of $\{X_{i,j}, QOX_{i,j}\}$ as current HM.

% End of quasi-oppositional generation jumping.

If NI is completed, return the best harmony vector X^{best} in the HM; otherwise go back to **Step 4.**

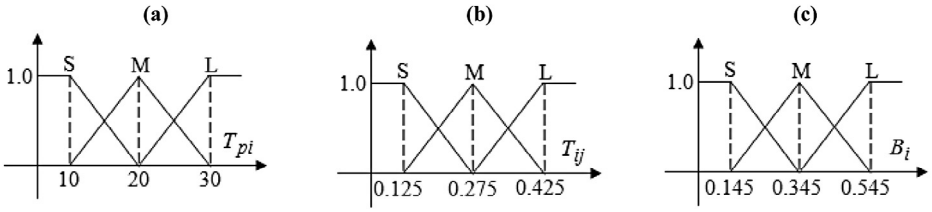

Fig. 4. Membership functions values: (a) T_{pi}, (b) T_{ij} and (c) B_i [35].

In the present work, a single environment (*i.e.* three area power system having six GENCOs/DISCOs) has been studied while considering the proposed QOHS as an optimizing tool. The effectiveness of the proposed QOHS for some other environments may be found in References 27 and 35.

6. GA: basic concept

GA is a global search technique based on the operations observed in natural selection and genetics [36,37]. It is a numerical optimization algorithm capable of being applied to a wide range of optimization problems that guarantees the survival of the fittest. They operate on a population of current approximations *i.e.* the individuals initially drawn at random from which improvement is sought. Individuals are encoded as strings (chromosomes) constructed over some particular alphabet (*e.g.* the binary alphabet (0, 1)) which uniquely mapped onto the decision variable domain. Once the decision variable domain representation of the current population is calculated, individual performance is assumed according to the objective function which characterizes the problem to be solved.

Genetic operators may be divided into three main steps [38] *viz.* (a) reproduction, (b) crossover and (c) mutation.

Table 1
Benchmark functions [39,40].

Benchmark functions	n	Search space	Global minimum [41]
$f_1(x)=\sum_{i=1}^{n-1}\left(100\left(x_{i+1}-x_i^2\right)\right)^2+(x_i-1)^2$	30	$[-30,30]^n$	0
$f_2(x)=\sum_{i=1}^{n}\left(\sum_{j=1}^{i}x_j\right)^2$	30	$[-100,100]^n$	0
$f_3(x)=\sum_{i=1}^{n}([x_i+0.5])^2$	30	$[-100,100]^n$	0
$f_4(x)=4x_1^2-2.1x_1^4+\frac{1}{3}x_1^6+x_1x_2-4x_2^2-4x_2^4$	2	$[-5,5]^n$	−1.0316285
$f_5(x)=\max_j\{\lvert x_i\rvert, 1\le i\le n\}$	30	$[-100,100]^n$	0

Step (a)	*Reproduction*: It selects the fittest individuals from the current population that may be used in generating the next population.
Step (b)	*Crossover:* It causes pairs or larger groups of individuals to exchange genetic information with one another.
Step (c)	*Mutation*: It causes individual genetic representations to be changed according to some probabilistic rule.

7. SFL based on-line tuning of PID controller gains

The whole process of SFL involves three main steps. These three steps are presented below [35].

Step (a)	*Fuzzification of input parameters*: Input parameters, such as T_p, T_{12} and B form fuzzy subsets like "small (S)", "medium (M)" and "large (L)" associated with the overlapping (between "S" and "M" or "M" and "L") triangular membership functions. The respective nominal central values of the subsets for T_p are (10, 20 and 30), those for T_{12} are (0.125, 0.275 and 0.425) and for B are (0.145, 0.345 and 0.545) at which membership value is unity. SFL rule base table consists of $3^3(=27)$ logical input conditions or sets (SFL tables calculated for different PID structures investigated), each composed of three nominal parameters. Each input set corresponds to nominal optimal gains as output. The limits of these subsets are featured in Fig. 4.
Step (b)	*Sugeno fuzzy interface:* For on-line, imprecise values of input parameters, fuzzy subset values are evaluated with the help of "IF", "THEN" logic and the corresponding membership values are determined from the membership functions of the subsets. For each input set, three membership values (*i.e.* T_p, T_{12} and B) and their minimum ($\mu_{\min}$) are computed.
Step (c)	*Sugeno defuzzification*: SFL yields the defuzzified crisp output for each gain. The final crisp output gain may be stated by equation (24)

$$K_{crisp}=\frac{\sum_i \mu_{\min}^i K_i}{\sum_i \mu_{\min}^i} \tag{24}$$

where i corresponds to input logical sets, K_i is nominal K_p or K_i or K_d. In equation (24), K_{crisp} is either K_p or K_i or K_d whereas $\mu_{\min}^i$ is the minimum membership value for the ith logical set being satisfied.

Table 2
Comparison of different algorithms, mean and standard deviation for benchmark functions.

Algorithm	Measure	$f_1(x)$	$f_2(x)$	$f_3(x)$	$f_4(x)$	$f_5(x)$
GA [40]	Mean	338.5516	9749.9145	3.697	−1.0298	7.9610
	Std.	361.497	2594.9593	1.9517	3.1314×10^{-3}	1.5063
PSO [40]	Mean	37.3582	1.1979×10^{-3}	0.146	−1.0160	0.4123
	Std.	32.1436	2.1109×10^{-3}	0.4182	1.2786×10^{-2}	0.2500
GSO [40]	Mean	49.8359	5.7829	1.6000×10^{-2}	−1.031628	0.1078
	Std.	30.1771	3.6813	0.1333	0	3.9981×10^{-2}
CQGSO [39]	Mean	34.4281	0.0404	0.0040	NaN	NaN
	Std.	24.5366	0.0291	0.0015	NaN	NaN
RCGA-RTVM [41]	Mean	28.988454719	7.5456×10^{-242}	0.0002	−1.0316284535	7.4950×10^{-24}
	Std.	0.6739399580	0	0.0141421356	2.8796×10^{-11}	1.0434×10^{-23}
QOHS [Proposed]	Mean	26.1428	6.1714×10^{-245}	0.0001	−1.0112	6.1211×10^{-25}
	Std.	0.5114	0	0.0112	2.1458×10^{-12}	1.0112×10^{-24}

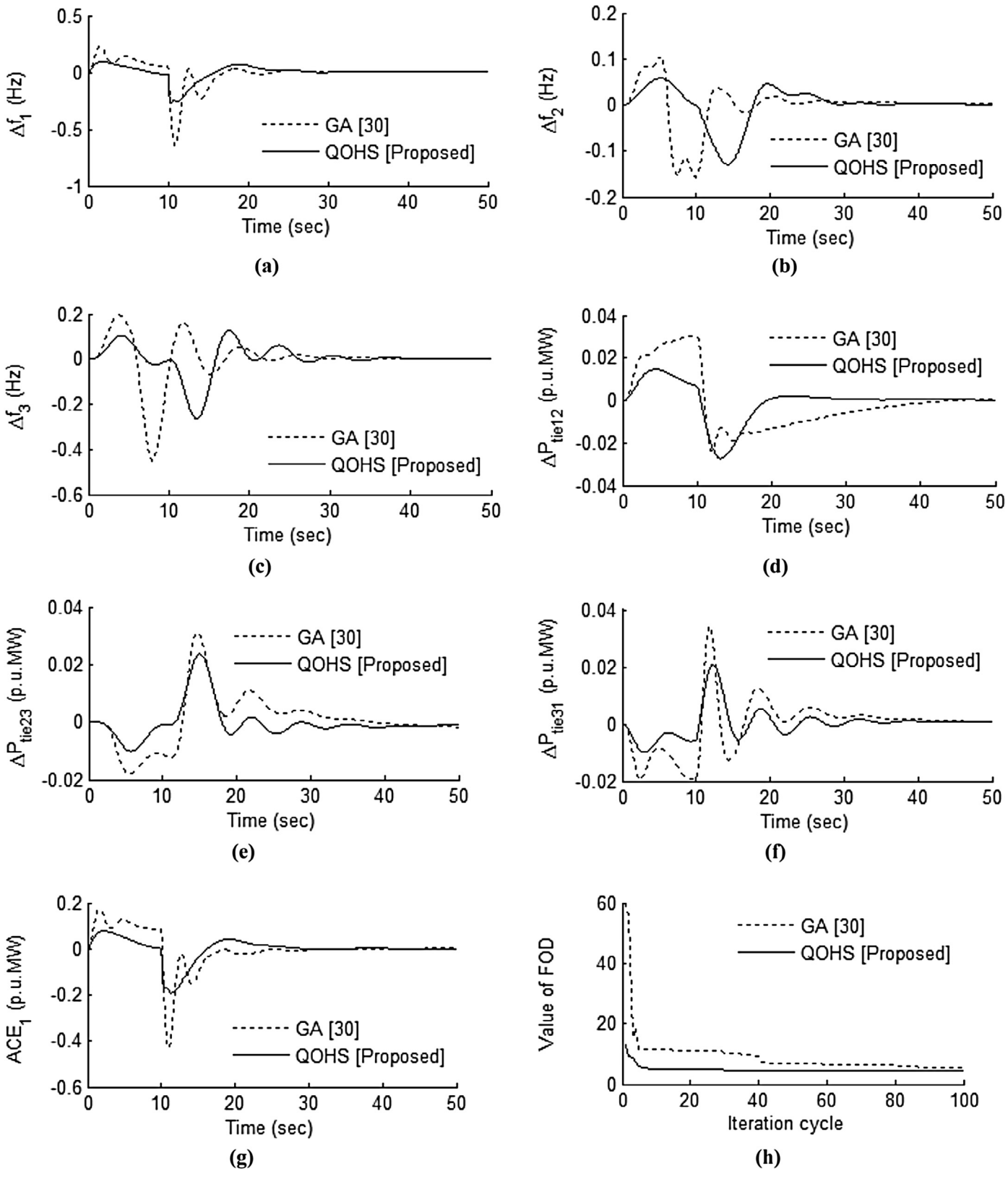

Fig. 5. Comparative GA and QOHS based AGC response profiles of the studied deregulated three-area test power system for the analyzed unilateral transaction case: (a) Δf_1, (b) Δf_2, (c) Δf_3, (d) ΔP_{tie12}, (e) ΔP_{tie23}, (f) ΔP_{tie31}, (g) ACE_1 and (h) convergence profile of *FOD*.

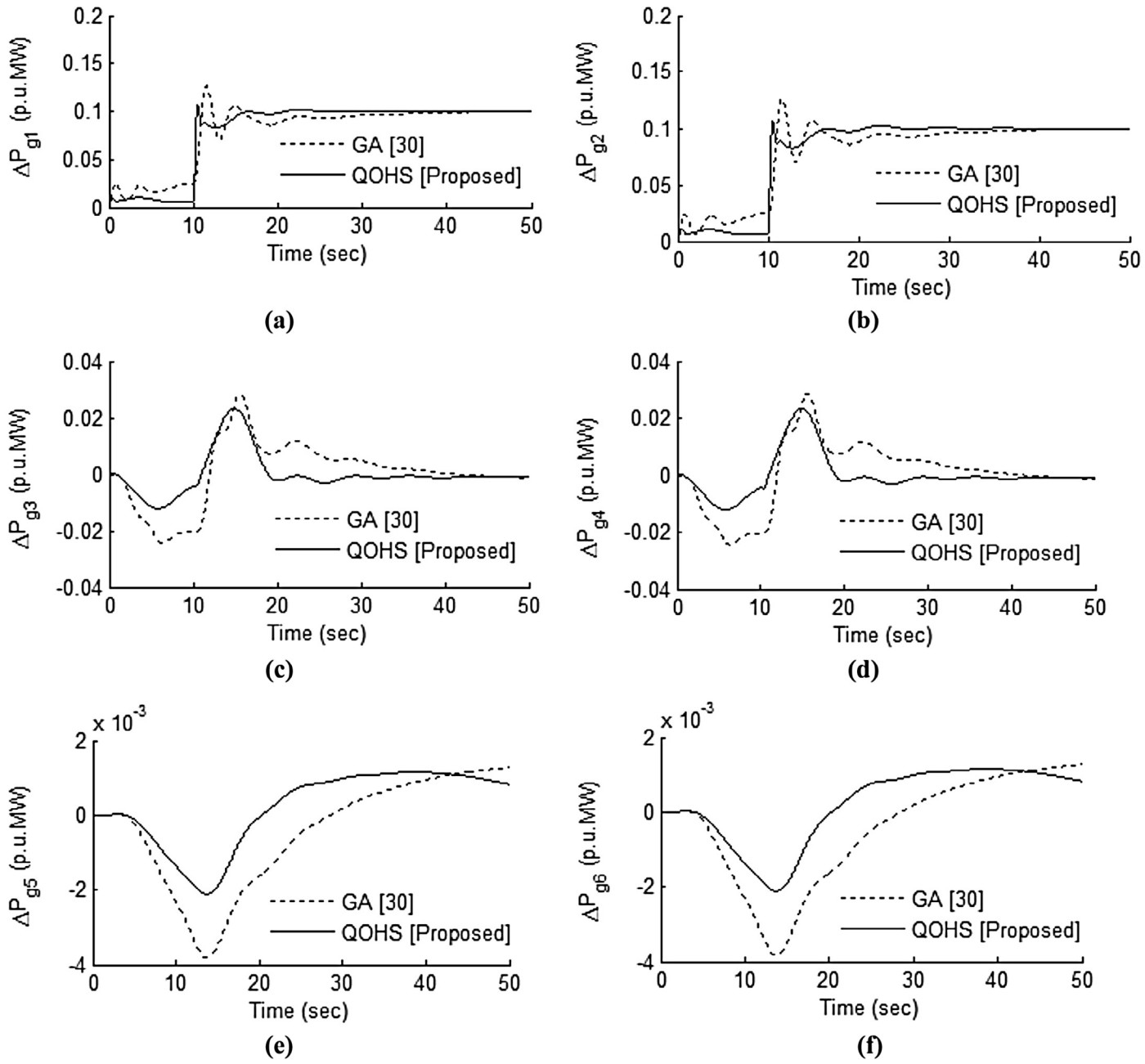

Fig. 6. Comparative GA and QOHS based generated profiles of each GENCO of the studied deregulated three-area test power system for the analyzed unilateral transaction case: (a) ΔP_{g1}, (b) ΔP_{g2}, (c) ΔP_{g3}, (d) ΔP_{g4}, (e) ΔP_{g5} and (f) ΔP_{g6}.

In the present work, Sugeno fuzzy rule base tables (not shown) are obtained by applying the proposed QOHS for distinct 27 number nominal input operating conditions. The outputs are 27 distinct nominal optimal AGC parameter sets.

8. Simulation results and discussion

8.1. QOHS for benchmark functions

In this section, the proposed QOHS is tested on a set of five benchmark functions in order to validate the performance of the algorithm. Descriptions of these benchmark functions [39,40] are presented in Table 1. The proposed QOHS is applied to these benchmark functions and, correspondingly, mean and standard deviations of the results are presented in Table 2. In this test, all the functions are tested on 100 dimensions and population size is 60. The number of iteration cycle is 100. The obtained results are compared with the results obtained by using GA [39], PSO [39], group search optimizer (GSO) [39], continuous quick GSO (CQGSO) [39] and real coded GA approach with random transfer vector-based mutation (RCGA-RTVM) [41]. It is clear from this table that the proposed QOHS converges to better results in comparison with GA, PSO, GSO and CQGSO and RCGA-RTVM algorithms.

8.2. QOHS for power system application

The proposed QOHS is used to evaluate a generating system characterized by deregulated three-area power system model with each

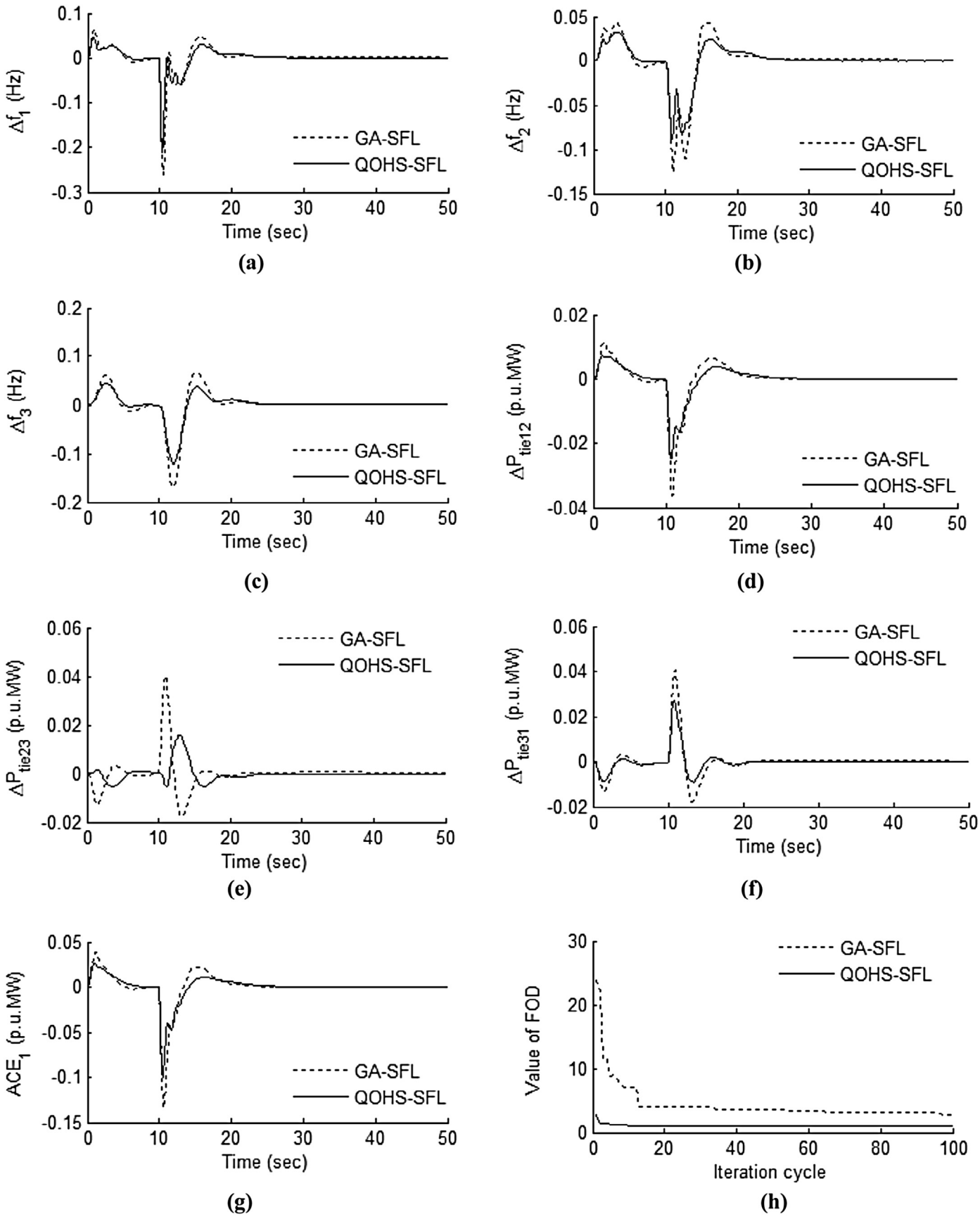

Fig. 7. Comparative GA-SFL and QOHS-SFL based AGC response profiles of the studied deregulated three-area power system model for the analyzed unilateral transaction case: (a) Δf_1, (b) Δf_2, (c) Δf_3, (d) ΔP_{tie12}, (e) ΔP_{tie23}, (f) ΔP_{tie31}, (g) ACE_1 and (h) convergence profile of *FOD*.

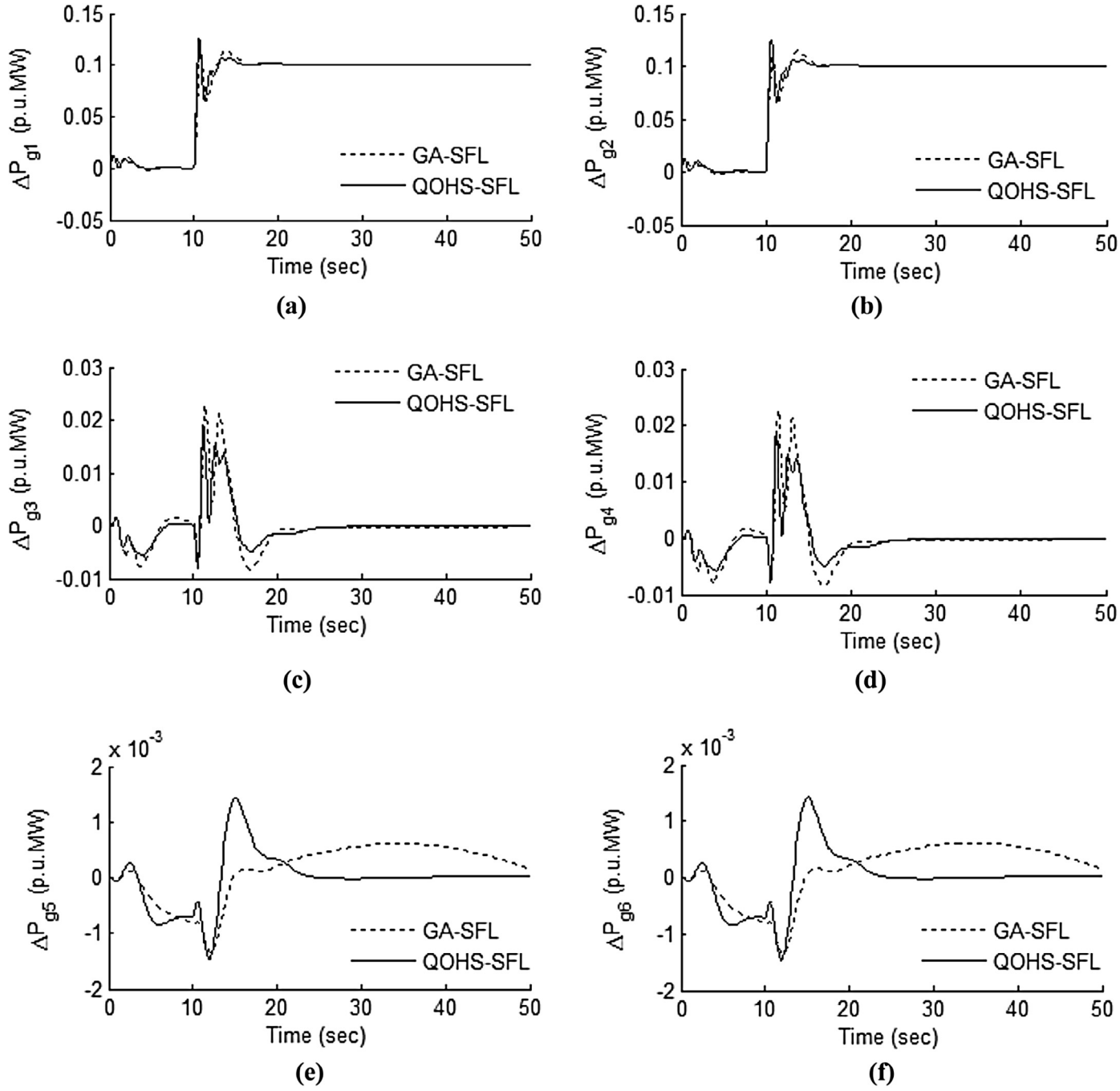

Fig. 8. Comparative GA-SFL and QOHS-SFL based generated profiles of each GENCO of the studied deregulated three-area test power system for the analyzed unilateral transaction case: (a) ΔP_{g1}, (b) ΔP_{g2}, (c) ΔP_{g3}, (d) ΔP_{g4}, (e) ΔP_{g5} and (f) ΔP_{g6}.

control area consisting of two GENCOs and two DISCOs (see Fig. 2). The relevant system parameters are included in the Appendix section for the simulated work. For the optimization, the proposed QOHS and the studied GA are adopted. GA is utilized for the sake of comparison purpose. The three cases of deregulated aspect which cover the major portion of the deregulation are discussed in this section. The major observations from the obtained results are discussed below. The results of interest are **bold faced** in their respective tables. The three cases considered are:

Case (a):	unilateral transaction,
Case (b):	bilateral transaction and
Case (c):	contract violation.

8.2.1. Case (a): unilateral transaction

In this case, the involvement of each GENCO is associated to its own area only. It may be the simplest case of power transaction in which the contribution of each GENCO is assumed to be equal [8]. Therefore, the values of *apf* must be the same for all the GENCOs (i.e. $apf_1 = apf_2 = apf_3 = apf_4 = apf_5 = apf_6 = 0.5$). It is assumed that area load changes occur in $DISCO_1$ only. The magnitude of this load demand is 0.1 p.u.MW. Conceptually, for GENCOs belonging to area-2 and area-3, the change in generated powers for each of them is equal to zero at the steady state condition. For this case study, DPM is initialized with the help of cpf_{11}, cpf_{12}, cpf_{21} and cpf_{22}. All these values are equal to 0.5.

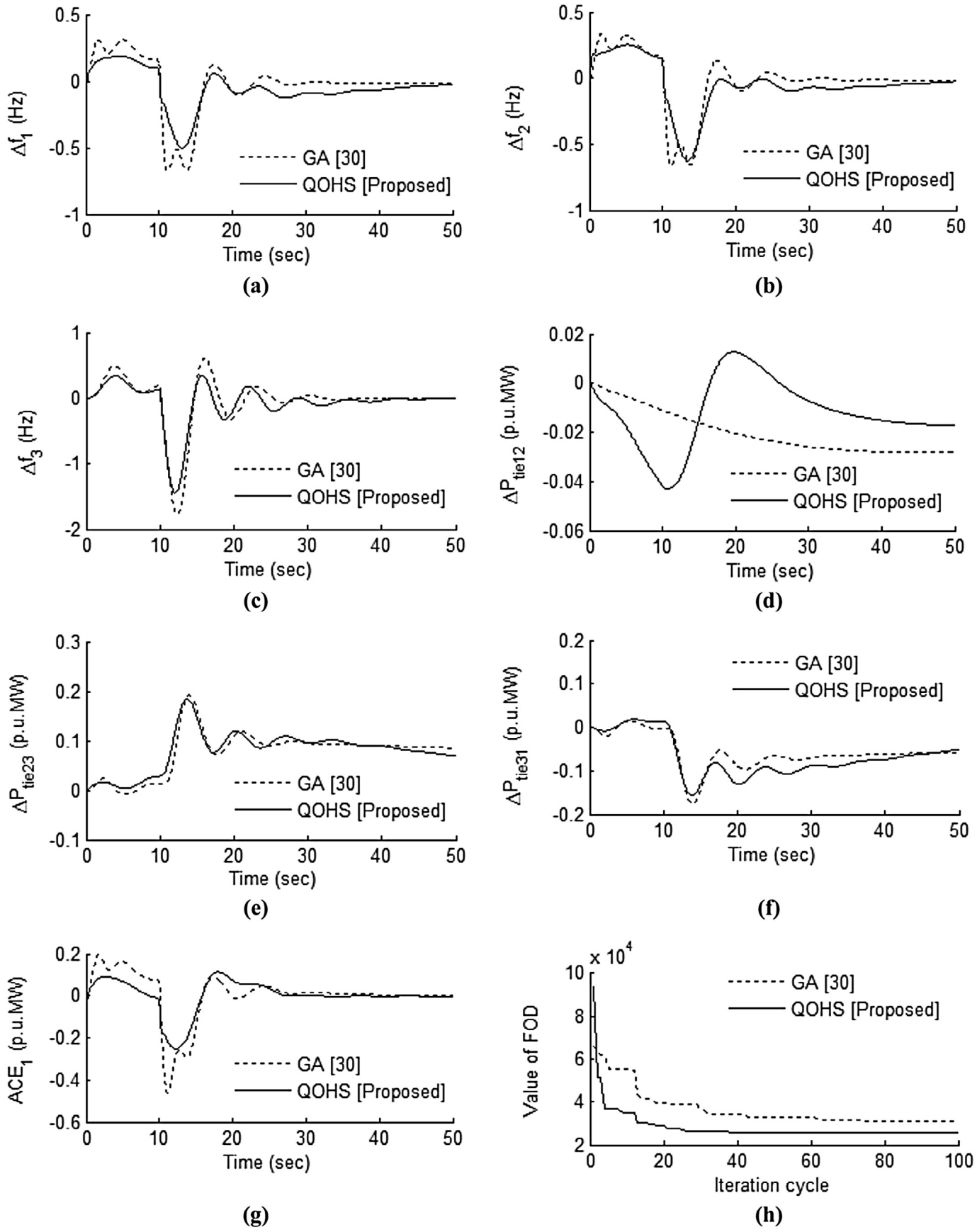

Fig. 9. Comparative GA and QOHS based AGC response profiles of the studied deregulated three-area power system model for the analyzed bilateral transaction case: (a) Δf_1, (b) Δf_2, (c) Δf_3, (d) ΔP_{tie12}, (e) ΔP_{tie23}, (f) ΔP_{tie31}, (g) ACE_1 and (h) convergence profile of *FOD*.

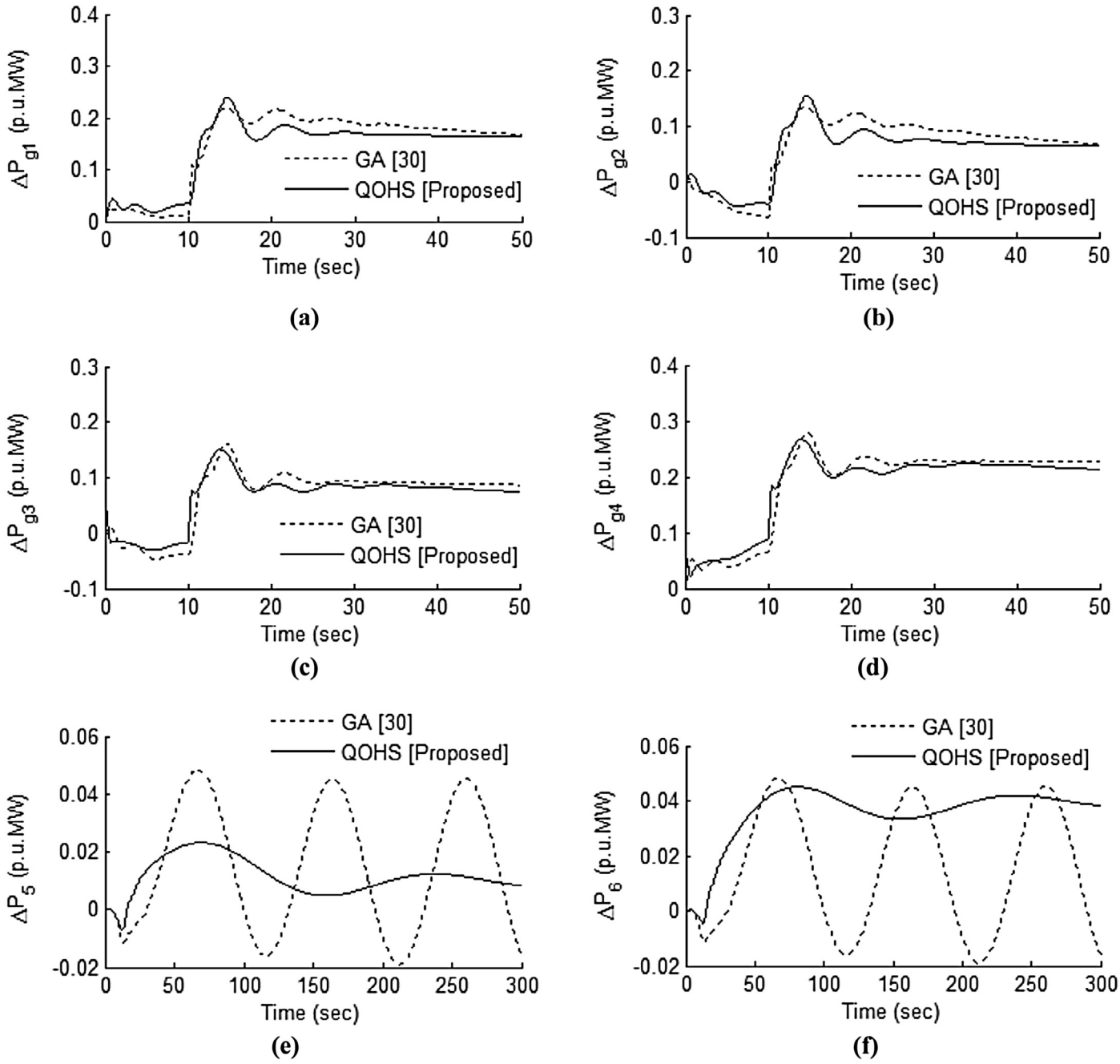

Fig. 10. Comparative GA and QOHS based generated profiles of each GENCO of the studied deregulated three-area test power system for the analyzed bilateral transaction case: (a) ΔP_{g1}, (b) ΔP_{g2}, (c) ΔP_{g3}, (d) ΔP_{g4}, (e) ΔP_{g5} and (f) ΔP_{g6}.

Figs. 5 and 6 show the comparative analysis of the studied GA and the proposed QOHS concerning to the unilateral transaction case study. In Fig. 5, the frequency deviations of area-1, area-2 and area-3, tie-line power deviations of area-(1-2), area-(2-3) and area-(3-1), amount of error in control area-1 and the convergence profile of FOD are shown. From the sub-section of Fig. 5a–c, it may be observed that QOHS based frequency deviation profiles tend to zero with small oscillations during the transient state. From Fig. 5d–f, QOHS based scheduled steady state power flow in the tie-lines are zero as there is no contract of power of a GENCO in one area to a DISCO of another area. Also, the average value of error in area-1 is minimized with the QOHS based controller (refer to Fig. 5g). The convergence profile of FOD, as yielded by the proposed QOHS, also shows the promising convergence characteristic (refer to Fig. 5h).

Fig. 6 shows the actual generated power profiles of each GENCO. From equation (3), the generated powers of each GENCO may be obtained as $\Delta P_{g1} = 0.1$ p.u.MW, $\Delta P_{g2} = 0.1$ p.u.MW, $\Delta P_{g3} = 0, \Delta P_{g4} = 0, \Delta P_{g5} = 0, \Delta P_{g6} = 0$. In the steady state, the generation of GENCOs match the demand of DISCOs in contract with it (refer to Fig. 6). Thus, the proposed QOHS based optimized PID controller gains provide more efficient dynamic responses as compared to GA.

In same sense, Figs. 7 and 8 show the comparative view of the GA-SFL and the QOHS-SFL techniques for on-line, off-nominal operating conditions in order to obtain the off-line dynamic responses. The obtained simulation results show that the utilization of SFL with the proposed QOHS is more effective in deregulated AGC system.

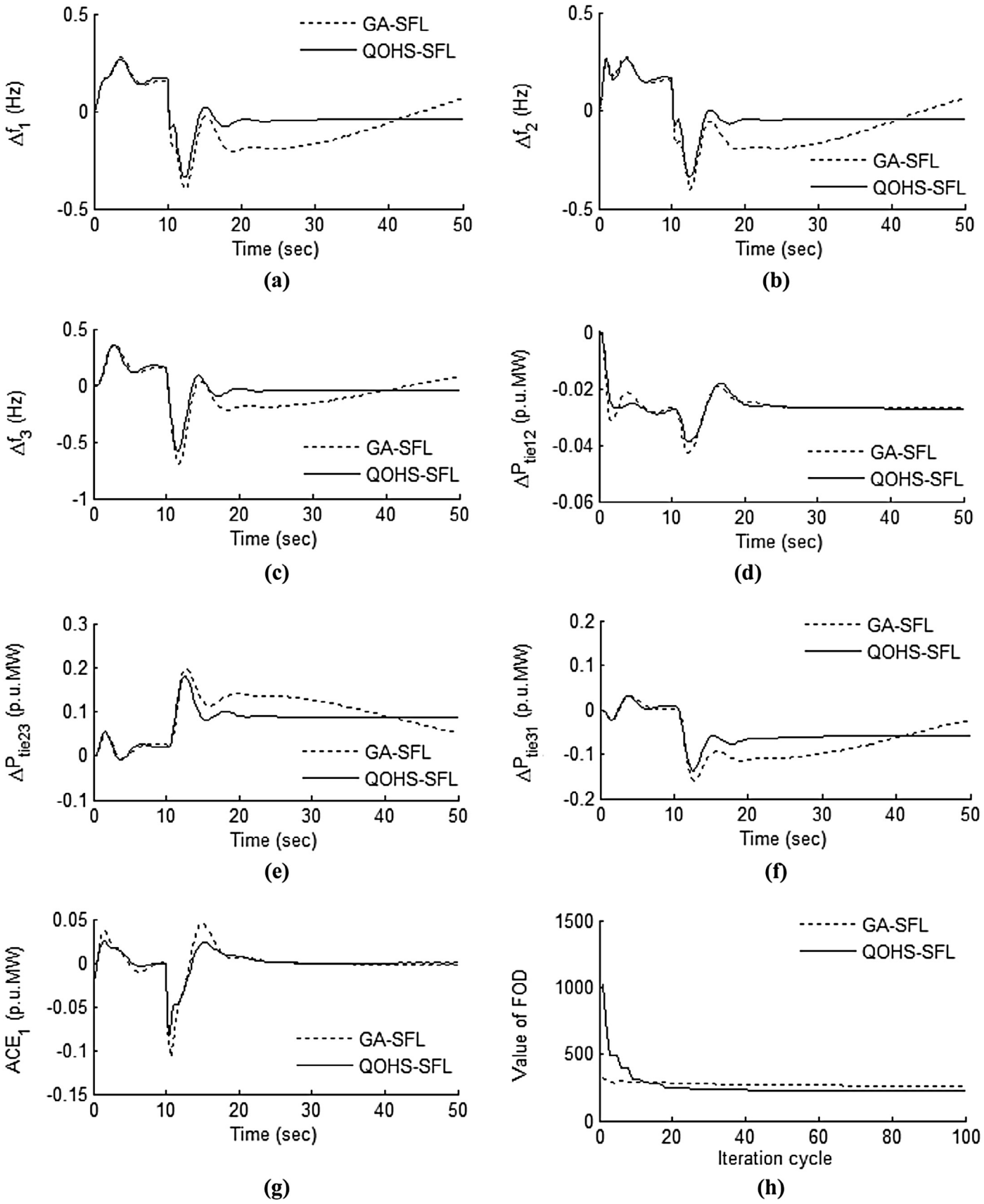

Fig. 11. Comparative GA-SFL and QOHS-SFL based AGC response profiles of the studied deregulated three-area power system model for the analyzed bilateral transaction case: (a) Δf_1, (b) Δf_2, (c) Δf_3, (d) ΔP_{tie12}, (e) ΔP_{tie23}, (f) ΔP_{tie31}, (g) ACE_1 and (h) convergence profile of *FOD*.

8.2.2. Case (b): bilateral transaction

In this kind of power transactions, GENCOs and DISCOs negotiate bilateral contracts among them and submit their contractual agreements to the ISO [3]. For this case study, it is assumed that each DISCO demands a load of 0.1 p.u.MW. The contribution of each GENCO of power system is assumed as $apf_1 = apf_2 = apf_3 = apf_4 = apf_5 = apf_6 = 0.5$. The significance of *apf* is to distribute the excess load in each GENCO as per specified value. As per this case study, the bilateral contracts are stated by equation (25).

$$\mathrm{DPM} = \begin{bmatrix} 0.3 & 0.25 & 0 & 0.4 & 0.1 & 0.6 \\ 0.2 & 0.15 & 0 & 0.2 & 0.1 & 0 \\ 0 & 0.15 & 0 & 0.2 & 0.2 & 0 \\ 0.2 & 0.15 & 1 & 0 & 0.2 & 0.4 \\ 0.2 & 0.15 & 0 & 0.2 & 0.2 & 0 \\ 0.1 & 0.15 & 0 & 0 & 0.2 & 0 \end{bmatrix} \quad (25)$$

Figs. 9 and 10 exhibit the overall view of the dynamic responses as offered by the studied GA and the proposed QOHS

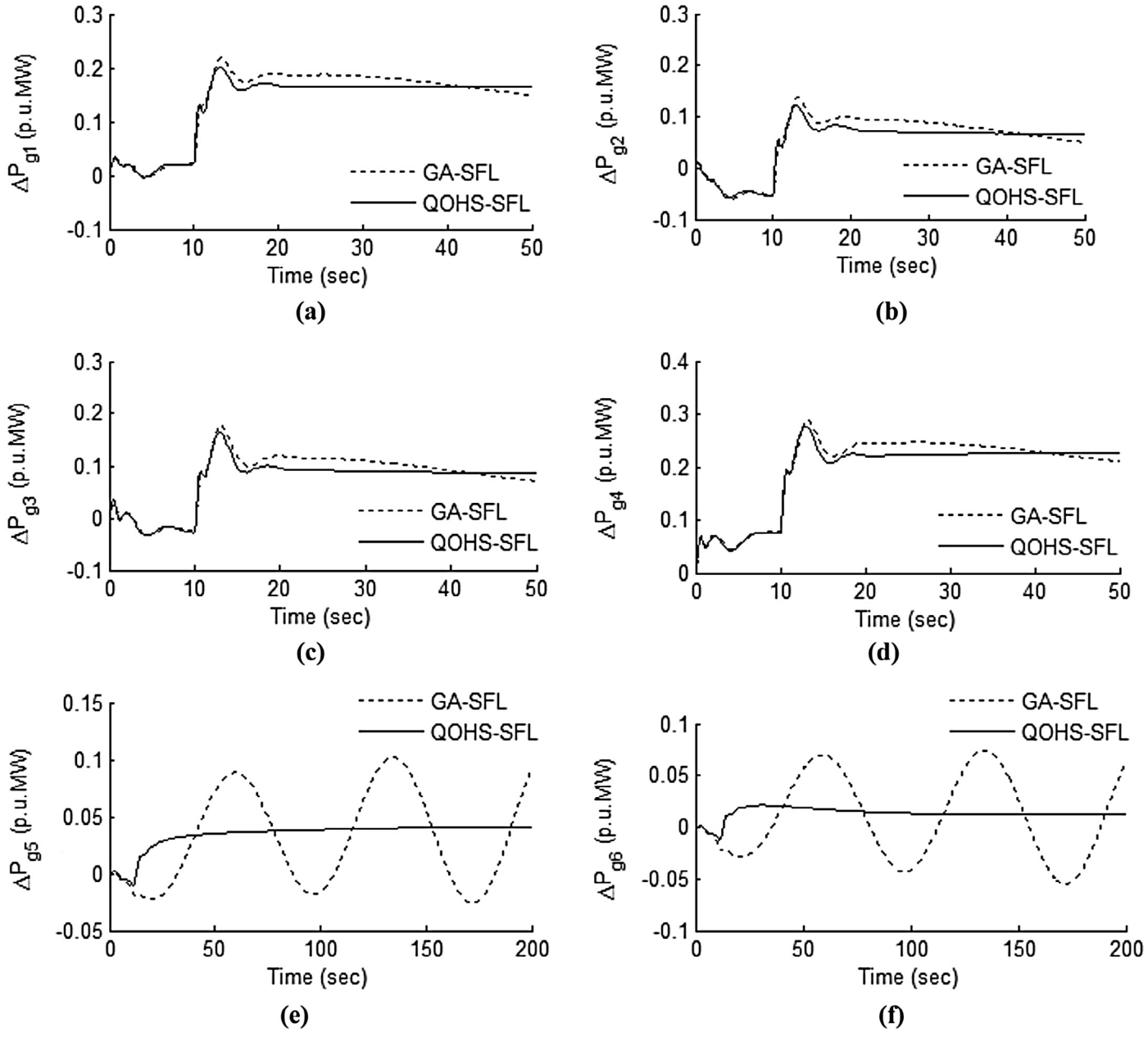

Fig. 12. Comparative GA-SFL and QOHS-SFL based generated profiles of each GENCO of the studied deregulated three-area test power system for the analyzed bilateral transaction case: (a) ΔP_{g1}, (b) ΔP_{g2}, (c) ΔP_{g3}, (d) ΔP_{g4}, (e) ΔP_{g5} and (f) ΔP_{g6}.

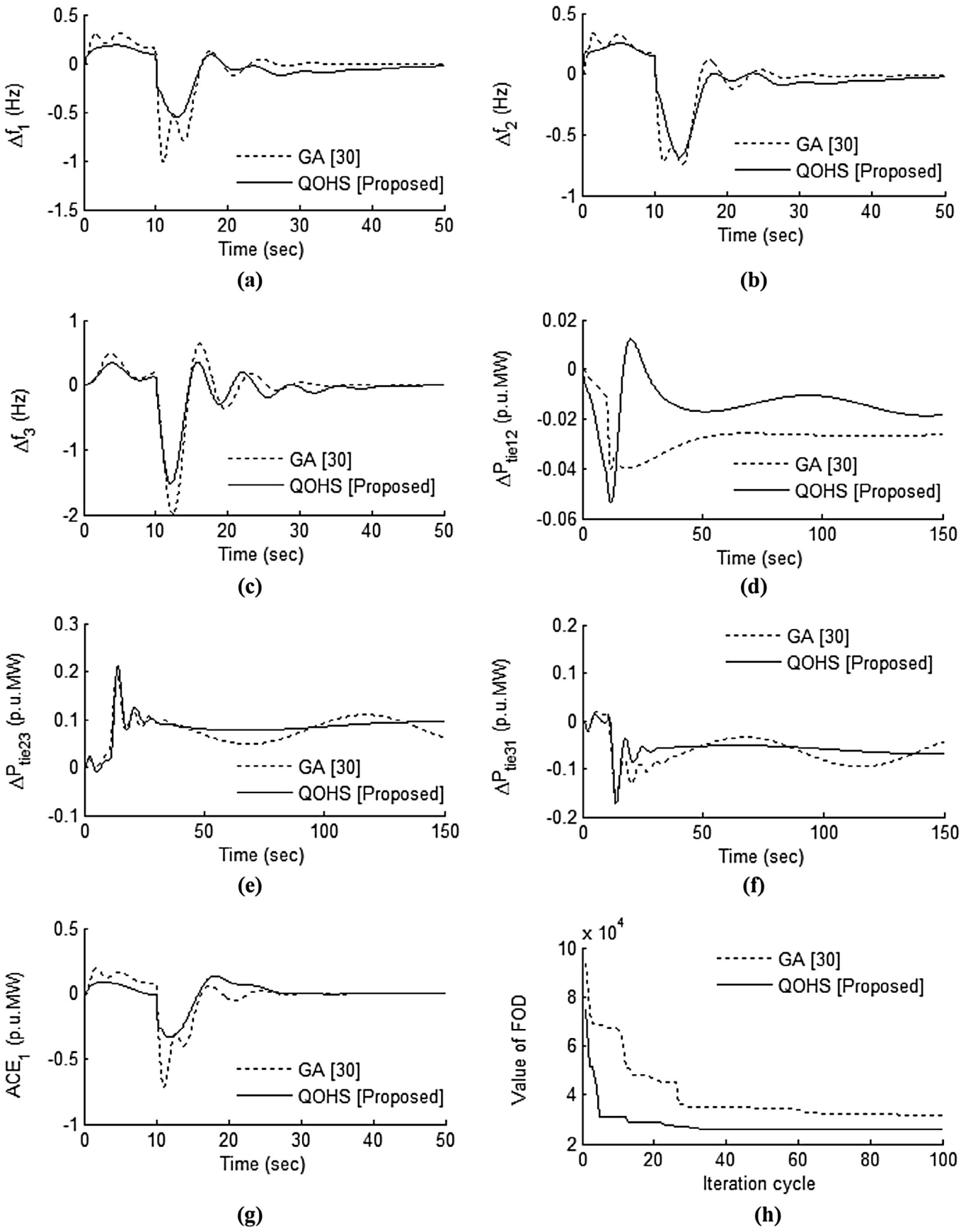

Fig. 13. Comparative GA and QOHS based AGC response profiles of the studied deregulated three-area power system model for the analyzed contract violation case: (a) Δf_1, (b) Δf_2, (c) Δf_3, (d) ΔP_{tie12}, (e) ΔP_{tie23}, (f) ΔP_{tie31}, (g) ACE_1 and (h) convergence profile of *FOD*.

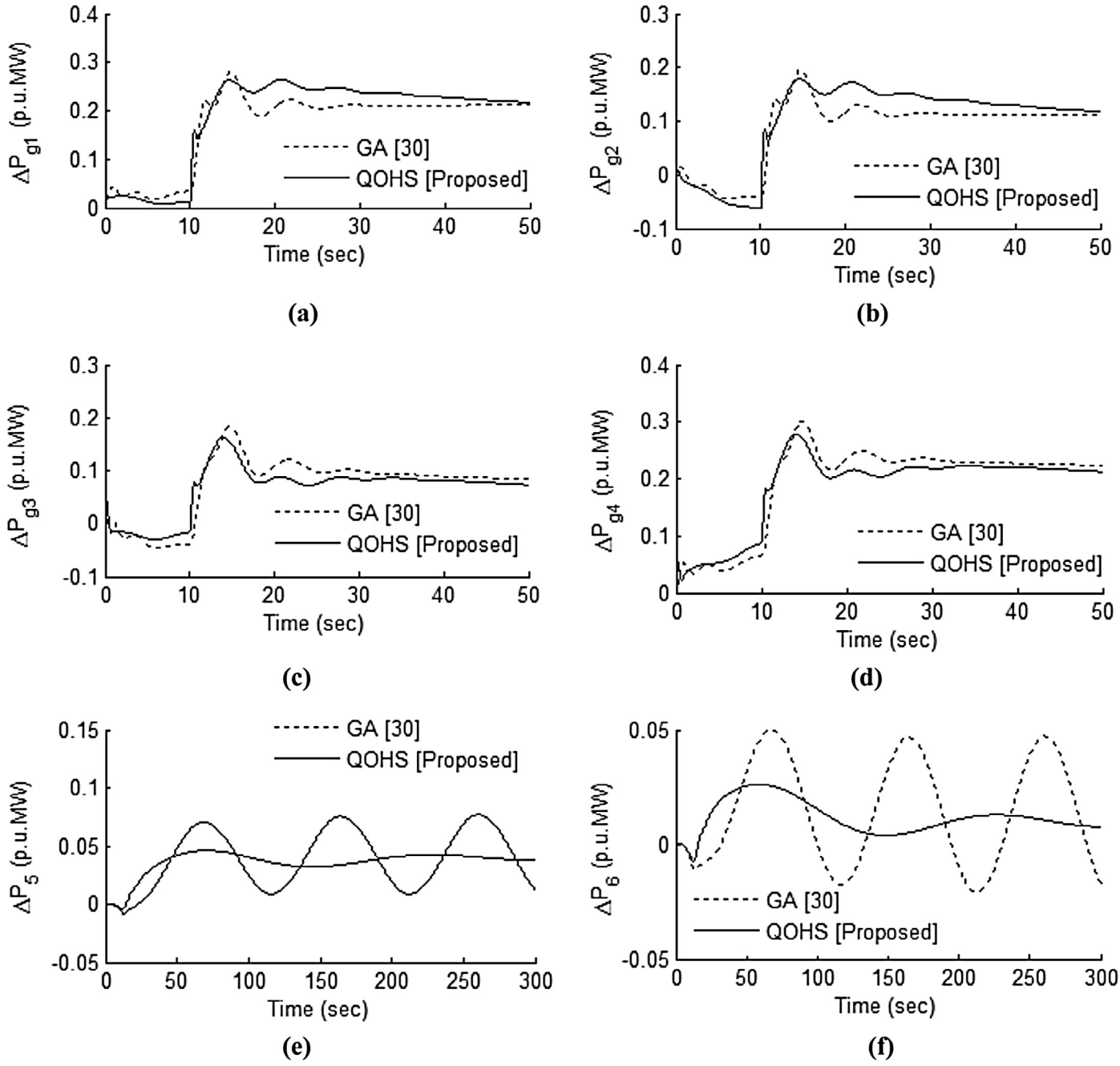

Fig. 14. Comparative GA and QOHS based generated profiles of each GENCO of the studied deregulated three-area test power system for the analyzed contract violation case: (a) ΔP_{g1}, (b) ΔP_{g2}, (c) ΔP_{g3}, (d) ΔP_{g4}, (e) ΔP_{g5} and (f) ΔP_{g6}.

under the study of bilateral transaction case. The response profiles as presented in this paper reveal that the proposed QOHS offers better dynamic responses and reaches their steady state values in a lesser time as compared to GA. Therefore, it may signify that the proposed QOHS acts as a better optimizing tool than the GA for the enhancement of deregulated AGC prospects.

From equation (3), the calculated generated powers of each GENCO are $\Delta P_{g1} = 0.165$ p.u.MW, $\Delta P_{g2} = 0.065$ p.u.MW, $\Delta P_{g3} = 0.055$ p.u.MW, $\Delta P_{g4} = 0.195$ p.u.MW, $\Delta P_{g5} = 0.075$ p.u.MW and $\Delta P_{g6} = 0.045$ p.u.MW. The scheduled steady state powers in the tie-lines may be calculated by equations (26) to (28).

$$\Delta P_{12(Scheduled)} = \sum_{i=1}^{i=2}\sum_{j=3}^{4} cpf_{ij}\Delta P_{Lj} - \sum_{i=3}^{4}\sum_{j=1}^{2} cpf_{ij}\Delta P_{Lj} = 0.01\ \text{p.u.MW} \quad (26)$$

$$\Delta P_{23(Scheduled)} = \sum_{i=3}^{i=4}\sum_{j=5}^{6} cpf_{ij}\Delta P_{Lj} - \sum_{i=5}^{6}\sum_{j=3}^{4} cpf_{ij}\Delta P_{Lj} = 0.06\ \text{p.u.MW} \quad (27)$$

$$\Delta P_{31(Scheduled)} = \sum_{i=5}^{i=6}\sum_{j=1}^{2} cpf_{ij}\Delta P_{Lj} - \sum_{i=1}^{2}\sum_{j=5}^{6} cpf_{ij}\Delta P_{Lj} = -0.02\ \text{p.u.MW} \quad (28)$$

In addition to QOHS, additionally, the QOHS-SFL technique is also applied to investigate its suitability in deregulated AGC system during

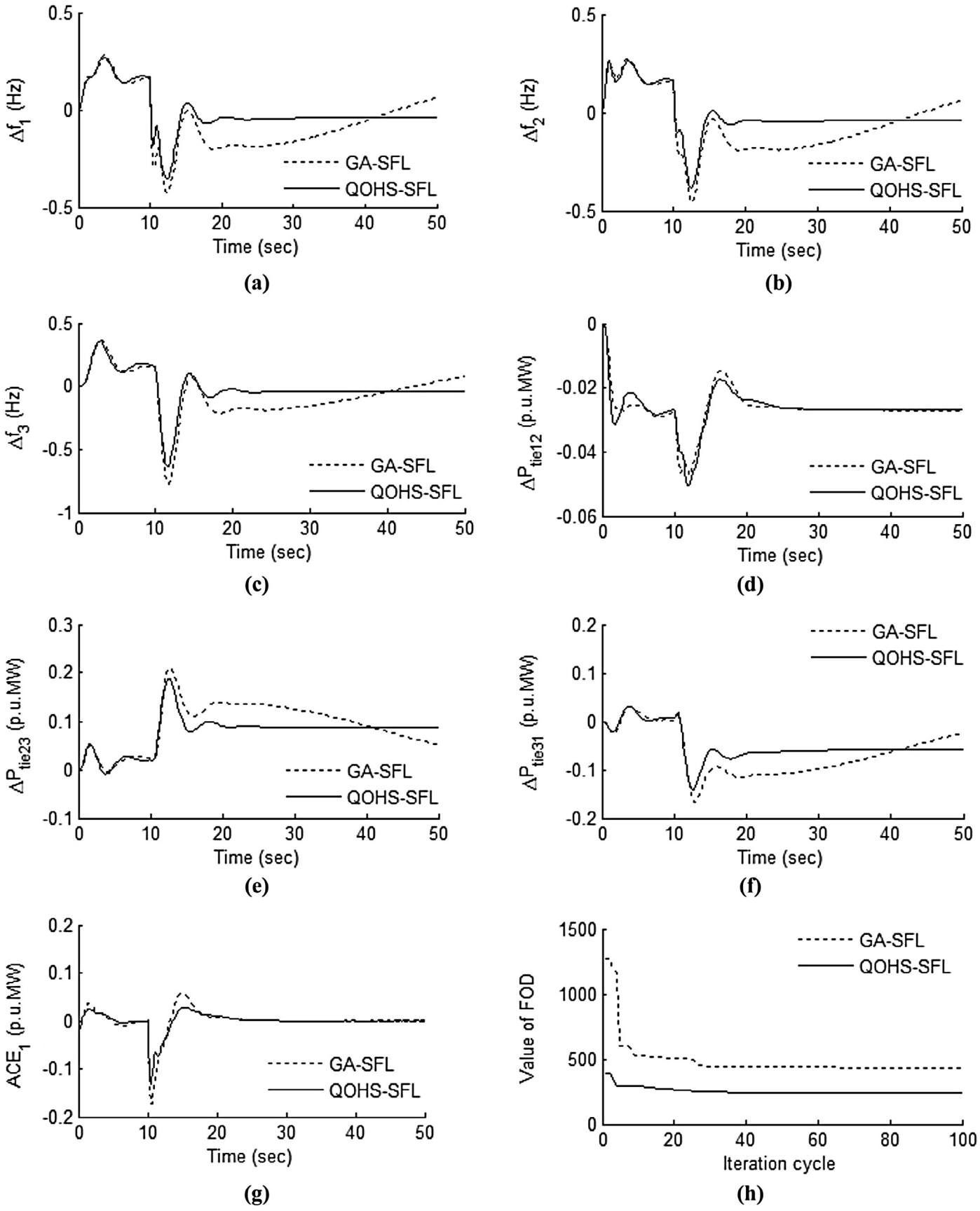

Fig. 15. Comparative GA-SFL and QOHS-SFL based AGC response profiles of the studied deregulated three-area test power system for the analyzed contract violation case: (a) Δf_1, (b) Δf_2, (c) Δf_3, (d) ΔP_{tie12}, (e) ΔP_{tie23}, (f) ΔP_{tie31}, (g) ACE_1 and (h) convergence profile of *FOD*.

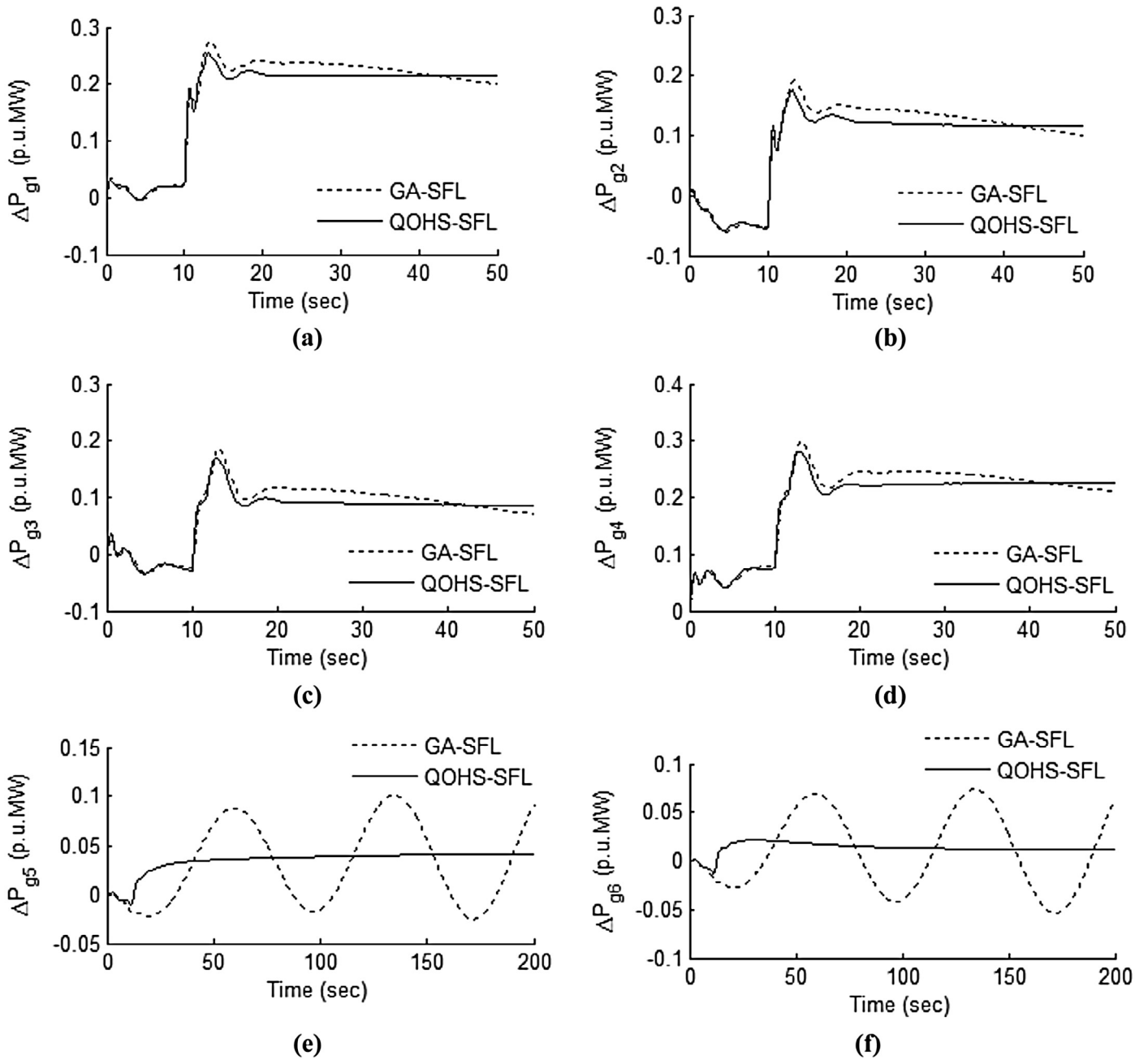

Fig. 16. Comparative GA-SFL and QOHS-SFL based generated profiles of each GENCO of the studied deregulated three-area test power system for the analyzed contract violation case: (a) ΔP_{g_1}, (b) ΔP_{g_2}, (c) ΔP_{g_3}, (d) ΔP_{g_4}, (e) ΔP_{g_5} and (f) ΔP_{g_6}.

on-line, off-nominal operating conditions. Figs. 11 and 12 portray the comparative GA-SFL and QOHS-SFL techniques based on obtained dynamic response profiles. These results clearly exhibit that for on-line, off-nominal operating conditions, the proposed QOHS-SFL technique shows significant improvement in dynamic response plots as compared to GA-SFL. Moreover, the generated profiles of each GENCO reached their scheduled value in the steady state. Hence, the proposed QOHS as well as QOHS-SFL technique is suitable for the optimization of PID controller gains concerning load following issues in deregulated bilateral power market.

8.2.3. Case (c): contract violation

In addition to the specified contracted load demands, there are un-contracted load demands than their specified ones for the DISCOs. At this condition, the agreement is violated [19]. In the present study, the AGC performance is tested in the presence of un-contracted load demands in addition to the specified contracted load demands. Consider again Case (b) with the assumption that $DISCO_1$ violates the contractual agreement by setting its *cpf* by demanding an excess power of 0.1 p.u.MW in area-1. However, it keeps the same *apf* as stated in Case (b). In this case, the total local demands in area-1 (ΔP_{L1}) is equal to the sums of load of $DISCO_1$ and $DISCO_2$ (*i.e.* $\Delta P_{L1} = (0.1+0.1) + 0.1$ p.u.MW $= 0.3$ p.u.MW). Similarly, the total local demand in area-2 (ΔP_{L2}) is equal to the sum of loads of $DISCO_3$ and $DISCO_4$ (*i.e.* $\Delta P_{L2} = 0.2$ p.u.MW). The total load in area-3 is the same as that of area-2. This excess load must be counted as a local load of area-1. This case study is based on the premises that ACE is an integral part of the control error feedback to GENCOs. If the

Table 3
Optimized PID controller gains for the studied deregulated three-area test system.

Algorithms	K_p (-ve)			K_i (-ve)			K_d (-ve)		
	Area-1	Area-2	Area-3	Area-1	Area-2	Area-3	Area-1	Area-2	Area-3
GA [30]	–	–	–	0.0854	0.0885	0.0699	–	–	–
QOHS [Proposed]	0.2538	0.0169	0.0010	0.5262	0.0010	0.2199	1.9510	1.7222	0.0170

An entry "–" means not applicable.

excess demand is not contracted out to any GENCO, the change in load appears only in terms of ACE. Hence, the additional demand of the shortfall of generation is shared by all the GENCOs of the area in which the contract violation occurs. Analytically, the GENCOs of area-1 (namely, $GENCO_1$ and $GENCO_2$) must respond to minimize this ACE signal.

Figs. 13 and 14 show the comparative analysis of GA and QOHS based dynamic response profiles. From these figures, it may be observed that the proposed QOHS based scheme achieves much better damping for frequency and tie-line power flow deviation profiles. As DPM is same to that of Case (b), the steady state tie-line power deviations are same as in Case (b). From equation (3), the generated powers of each GENCO may be calculated as $\Delta P_{g1} = 0.215$ p.u.MW $\Delta P_{g2} = 0.115$ p.u.MW, $\Delta P_{g3} = 0.055$ p.u.MW, $\Delta P_{g4} = 0.195$ p.u.MW, $\Delta P_{g5} = 0.075$ p.u.MW and $\Delta P_{g6} = 0.045$ p.u.MW. Moreover, the steady state generation of $GENCO_3$, $GENCO_4$, $GENCO_5$ and $GENCO_6$ is not affected by the excess load of $DISCO_1$. The un-contracted load of $DISCO_1$ is reflected in the generation of $GENCO_1$ and $GENCO_2$ (refer to Figs. 14a and b).

The same case is investigated for the studied GA-SFL and the proposed QOHS-SFL techniques for the studied model. The closed loop system behavior is tested through the same un-contracted load demand as studied earlier. The generated AGC profiles are shown in Figs. 15 and 16. It may be observed that the frequency deviations of all the controlled three areas are quickly driven back to zero with improved dynamic responses. It may be concluded that the proposed QOHS-SFL enhances the system damping characteristics in all the considered deregulated cases and a promising optimization technique.

For unilateral, bilateral based and the contract violation case, the optimized PID controller gains as obtained by the GA/QOHS and the proposed QOHS-SFL/GA-SFL are presented in Tables 3 and 4, in order. The FOD values corresponding to this are presented in Tables 5 and 6, in order. Examining Tables 5 and 6, it may be inferred that the proposed QOHS offers lower FOD value (for all the considered cases viz. Case (a), Case (b) and Case (c)) as compared to GA. The eigenvalues are also calculated for the proposed QOHS based controller in bilateral based scenario as stated in Table 7. Table 7 shows that there is a slight shift in the position of eigenvalues in all the examined cases (as presented in Figs. 16–19). This shows that the optimized controller gains produces satisfactory dynamic responses even wide change in system configuration. It may also be inferred that the performance of the proposed QOHS-PID controller produces satisfactory results. The simulation results show that the proposed QOHS tracks the load changes efficiently while tuning the PID controller gains.

8.2.4. Sensitivity analysis of three-area power system

Sensitivity analysis is carried out to study the uncertainty in dynamic behavior at nominal condition to wide change in some of the important parameters of the power system. The aim of this study is to examine the performance of the designed controller under these parameter variations. In this paper, sensitivity analysis is carried out by varying the operating load conditions, governor time-constant and turbine time-constant in the range of ±25% with nominal system parameter. The profiles of Δf_1, Δf_2 and ΔP_{tie12} pertaining to sensitivity analysis with change in rated load condition, governor

Table 4
SFL based optimized PID controller gains for the studied deregulated three-area test system.

Nominal input parameters T_{pi}, T_{ij}, B_i	Algorithms	K_p (-ve)			K_i (-ve)			K_d (-ve)		
		Area-1	Area-2	Area-3	Area-1	Area-2	Area-3	Area-1	Area-2	Area-3
24, 0.28, 0.32	GA-SFL	1.8561	1.8756	0.9383	2.5005	4.9805	0.3134	1.9342	1.9733	4.9805
	QOHS-SFL	4.0552	3.1997	0.0889	2.5632	10.4039	0.0735	3.0093	3.1142	19.9899

Table 5
Comparative GA and QOHS based performance indices of the studied deregulated cases for the three-area test system.

Studied algorithms	Case (a): Unilateral transaction				Case (b): Bilateral transaction				Case (c): Contract violation			
	FOD	ITAE	ITSE	IAE	FOD	ITAE	ITSE	IAE	FOD	ITAE	ITSE	IAE
GA [30]	1.32	94.69	14.21	7.88	13.26	100	100	29.86	16.58	100	100	32
QOHS [Proposed]	**0.51**	**72.62**	**6.42**	**5.297**	**8.94**	**94.51**	**89.5**	**25.39**	**10.06**	**96.23**	**91.3**	**29.51**

Table 6
Comparative GA-SFL and QOHS-SFL based performance indices of the studied deregulated cases for the three-area test system.

Studied algorithms	Case (a): Unilateral transaction				Case (b): Bilateral transaction				Case (c): Contract violation			
	FOD	ITAE	ITSE	IAE	FOD	ITAE	ITSE	IAE	FOD	ITAE	ITSE	IAE
GA-SFL	0.04	11.81	0.19	11.81	1.75	100	15.36	15.03	2.03	100	15.85	15.43
QOHS-SFL	**0.08**	**5.70**	**0.09**	**1.06**	**1.36**	**90**	**12.05**	**11.96**	**1.52**	**92**	**12.15**	**12.29**

Table 7
System eigenvalues under parameter variations with the bilateral based transaction.

ΔP_L		T_g		T_t	
−25%	+25%	−25%	+25%	−25%	+25%
−1.0000	−1.0000	−1.0000	−1.0000	−1.0000	−1.0000
−1.0000	−1.0000	−1.0000	−1.0000	−1.0000	−1.0000
−1.0000	−1.0000	−1.0000	−1.0000	−1.0000	−1.0000
−0.0648	−0.0648	−0.0704	−0.0605	−0.0712	−0.0613
−0.0638	−0.0638	−0.0694	−0.0596	−0.0701	−0.0605
−0.0039 ± 0.0214i	−0.0039 ± 0.0214i	−0.0045 ± 0.0216i	−0.0034 ± 0.0212i	−0.0057 ± 0.0222i	−0.0027 ± 0.0206*i*
−0.0064 ± 0.0191i	−0.0064 ± 0.0191i	−0.0071 ± 0.0192i	−0.0057 ± 0.0190i	−0.0087 ± 0.0197i	−0.0048 ± 0.0184*i*
−0.0333	−0.0333	−0.0333	−0.0333	−0.0444	−0.0267
−0.0333	−0.0333	−0.0333	−0.0333	−0.0444	−0.0096
−0.0018 ± 0.0086i	−0.0018 ± 0.0086i	−0.0018 ± 0.0086i	−0.0017 ± 0.0085i	−0.0018 ± 0.0087i	−0.0017 ± 0.0084*i*
−0.0104	−0.0104	−0.0107	−0.0101	−0.0115	−0.0267
−0.0200	−0.0200	−0.0200	−0.0200	−0.0200	−0.0200
−0.0500	−0.0500	−0.0571	−0.0444	−0.0500	−0.0500
−0.0500	−0.0500	−0.0571	−0.0500	−0.0500	−0.0500
−0.0200	−0.0200	−0.0200	−0.0200	−0.0200	−0.0200
−0.0041	−0.0041	−0.0042	−0.0041	−0.0042	−0.0041
0.0000 ± 0.0007i	0.0000 ± 0.0007i	−0.0015 ± 0.0003i	0.0000 ± 0.0007i	−0.0015 ± 0.0003i	−0.0015 ± 0.0003*i*
−0.0015 ± 0.0003i	−0.0015 ± 0.0003i	0.0000 ± 0.0007i	−0.0015 ± 0.0003i	0.0000 ± 0.0007i	0.0000 ± 0.0007*i*
−0.0016	−0.0016	−0.0016	−0.0016	−0.0016	−0.0016
−0.0002	−0.0002	−0.0002	−0.0002	−0.0002	−0.0002
−0.0010	−0.0010	−0.0010	−0.0010	−0.0010	−0.0010
−0.0010	−0.0010	−0.0010	−0.0010	−0.0010	−1.0000
−1.0000	−1.0000	−1.0000	−1.0000	−1.0000	−1.0000
−1.0000	−1.0000	−1.0000	−1.0000	−0.0010	−1.0000

time-constant and turbine time-constant are illustrated in Figs. 17–19, in order. It may be inferred from these figures that the proposed QOHS based PID controller gains provides a robust and stable speed control mechanism. The superiority of the proposed QOHS method is verified and the power system oscillations are effectively alleviated. Moreover, the tuned value of the controller gains obtained at the nominal loading with nominal parameters need not to be reset for wide change in the system configuration.

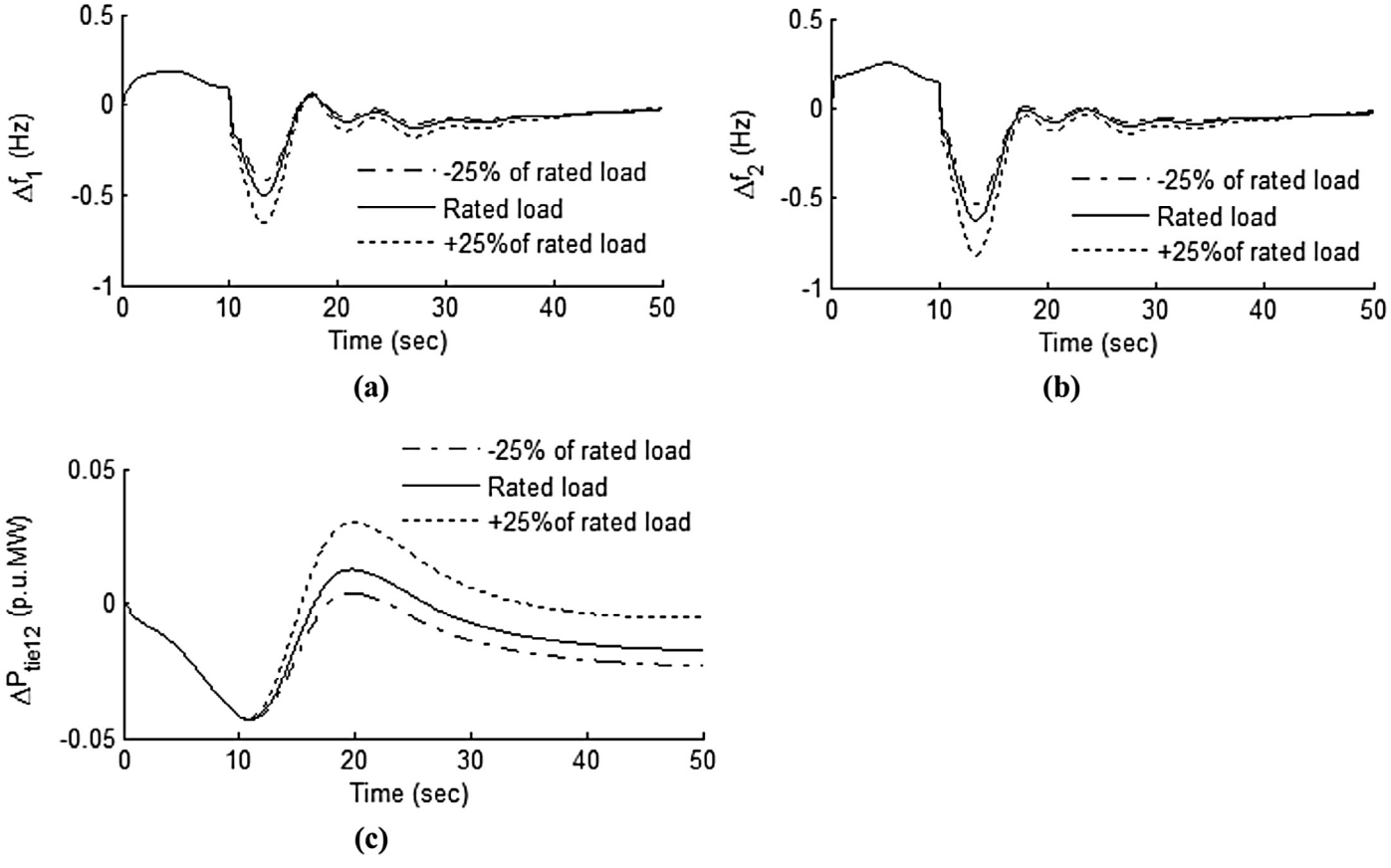

Fig. 17. Sensitivity analysis of the studied three-area test power system with change in rated load condition: (a) Δf_1, (b) Δf_2 and (c) ΔP_{tie12}.

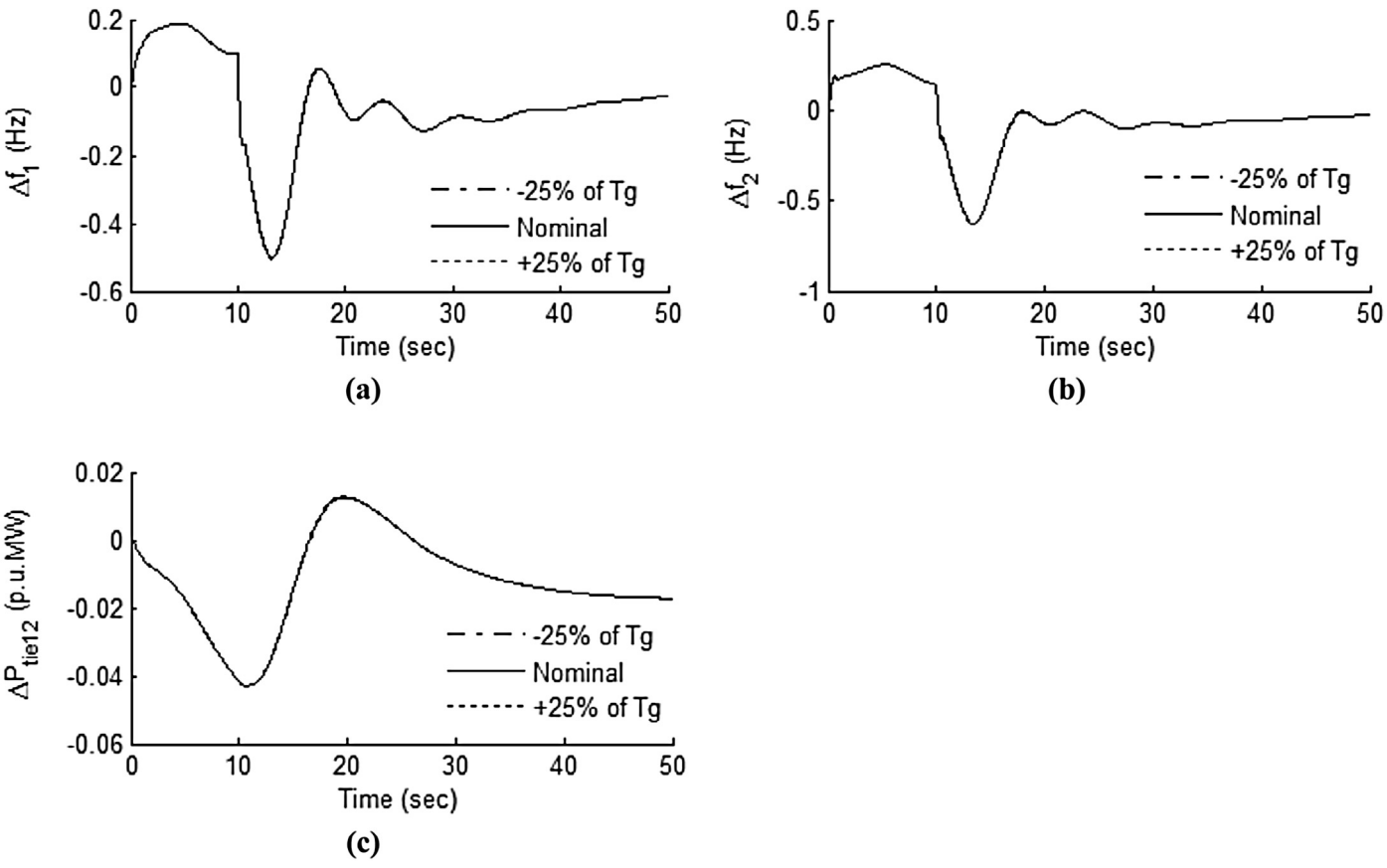

Fig. 18. Sensitivity analysis of the studied three-area test power system with change in governor time-constant: (a) Δf_1, (b) Δf_2 and (c) ΔP_{tie12}.

8.2.5. Computational cost analysis of the proposed QOHS

The analysis of an algorithm is related to the determination of the amount of resources (such as time and storage) necessary to execute them. Most algorithms are designed to work with inputs of arbitrary length. Usually, the efficiency or running time of an algorithm is stated as a function relating the input length to the number of steps or storage location. In the present study, the computational cost of the proposed QOHS is compared with the studied GA and is presented in Table 8. The comparative computational cost analysis is based on the same number of population (taken as 60) and the same number of iteration cycle (chosen as 100). From this table, it may be noted that the computational cost of the proposed QOHS is lower than the studied GA for the same chosen system configuration.

9. Conclusions

The test model of a three-area power system confined in deregulated AGC environment subjected to various uncertainties and load disturbances is studied in this paper. Considering the studied deregulated cases, the proposed QOHS is utilized for the design of controller gains by assuming all the interface variables such as control area frequencies, tie-line powers and all other possible contracts between GENCOs and DISCOs. Simulations are carried out on a three-area power system model. The simulated dynamic response profiles show that the proposed QOHS is compatible in deregulated AGC domain. It may be verified that the calculated generated powers of each GENCO matches with the generated response profiles for each case study. The results of sensitivity analysis also point out that the proposed QOHS based controller is a significant AGC tool in deregulated AGC domain. Therefore, the proposed QOHS may be a feasible and a relevant technique in comparison to tested GA for its utility in deregulated AGC study.

In the second phase of investigation, the benefits of the proposed QOHS-SFL technique is also demonstrated for the same studied test system. The presented work shows that the implementation of QOHS-SFL yields better AGC responses in comparison to tested GA-SFL in deregulated mode of operation. The obtained QOHS based FOD value also point out that the optimized PID controller gains are nearer to global optima, justified by promising convergence characteristic.

Table 8
Comparative study of computational cost of the studied algorithms.

Algorithms	Computational time (in seconds)
GA [30]	885.41
QOHS [Proposed]	**793.49**

AppendixPower system and algorithm parameter values

A.1 Parameters of deregulated three-area power system model [30]

$P_r = 2000$ MW (rated), $K_{p1,2} = 120$ Hz/p.u.MW, $T_{p1,2} = 20$ s, $K_{p3} = 80$ Hz/p.u.MW, $T_{p3} = 13$ s, $R_{1,2,3,4,5,6} = 2.4$ Hz/p.u.MW, $T_{t1,2,3,4} = 0.3$ s, $T_{g1,2,3,4} = 0.2$ s, $K_{r1,2,3,4} = 0.333$, $T_{r1,2,3,4} = 10$ s, $T_1 = T_4 = 48.7$ s, $T_2 = T_5 = 0.513$ s, $T_3 = T_6 = 10$ s, $T_w = 1$ s, $a_{12} = a_{23} = a_{31} = -1$,

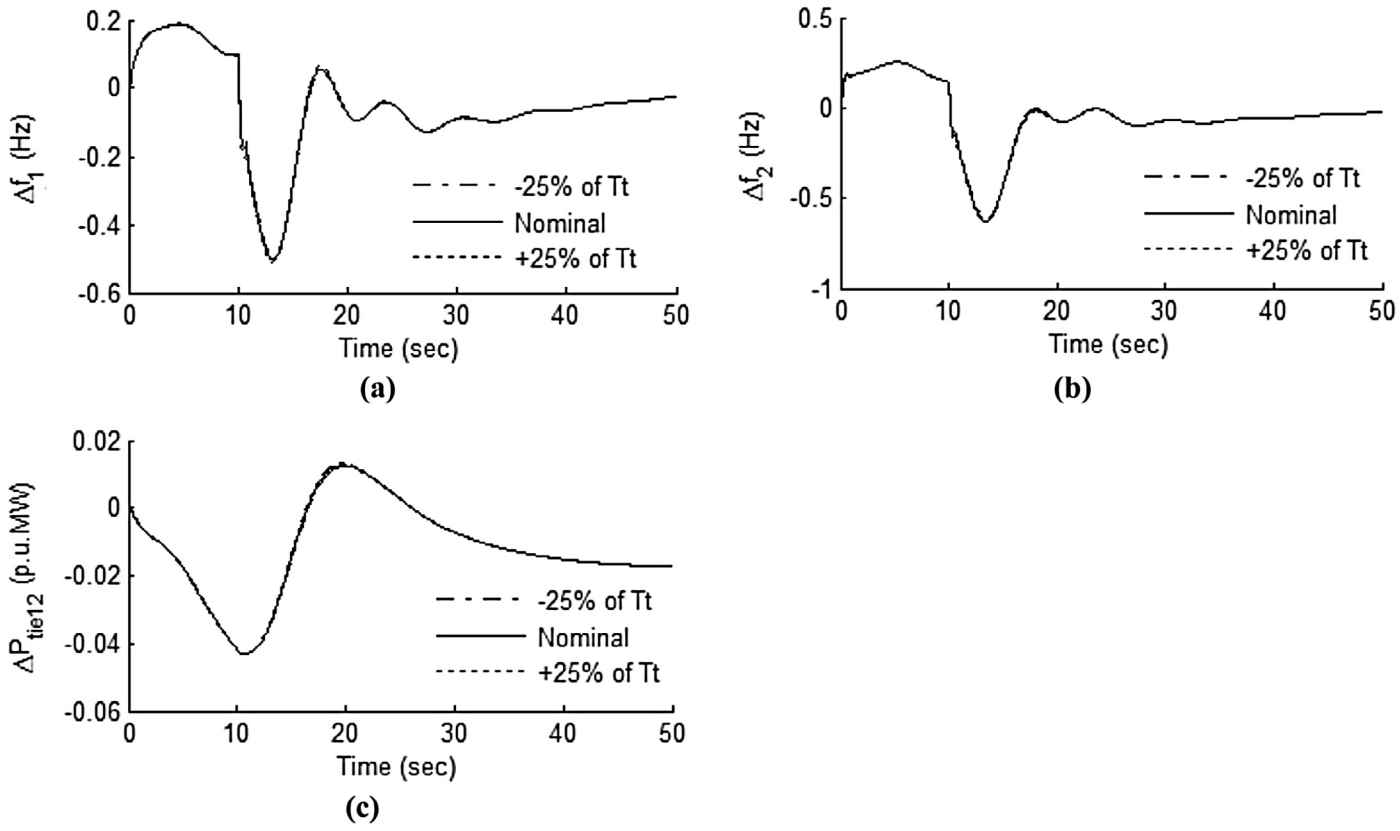

Fig. 19. Sensitivity analysis of the studied three-area test power system with change in turbine time-constant: (a) Δf_1, (b) Δf_2 and (c) ΔP_{tie12}.

$T_{ij} = 0.0707$, $T = 0.2$ s, $K_{I\max} = 0.2$, $K_{I\min} = 0.01$, $B_1 = 0.6476$, $B_2 = 0.6235$, $B_3 = 0.3657$, $B_{\max} = 2.35$, $B_{\min} = 0.005$.

A.2 Parameters of GA [30]

Number of parameters depends on problem variables (AGC configuration), number of bits = (number of parameters) × 8, population size = 50, maximum number of iteration cycles = 100, mutation rate = 0.04, crossover rate = 80%.

A.3 Parameters of QOHS

Number of parameters depends on problem variables (AGC configuration), population size = 50, maximum number of iteration cycle = 100, $HMCR = 0.9$, $PAR_{\min} = 0.45$, $PAR_{\max} = 0.98$, $BW_{\min} = 0.0005$, $BW_{\max} = 50$, $J_r = 0.8$.

A.4 Parameters for the deregulated three-area power system model with SFL technique

Parameters	Area-1	Area-2	Area-3
Governor regulation (R)	2.4	2.4	2.4
Governor time-constant (T_g)	0.2	0.2	0.2
Non-reheat turbine time-constant (T_t)	0.3	0.3	0.3
Reheat time-constant (T_r)	4.20	4.10	4.0
Reheat parameter (c)	0.34	0.31	0.32
Power system gain constant (K_p)	120.0	115.0	118.0
Power system time-constant (T_{pi})	(10-20-30)	(10-20-30)	(10-20-30)
Frequency bias constant (B_i)	(0.145-0.345-0.545)	(0.145-0.345-0.545)	(0.145-0.345-0.545)
Tie-line coefficient between area-1 and area-2 (T_{ij})	(0.125-0.275-0.425)	(0.125-0.275-0.425)	(0.125-0.275-0.425)

References

[1] O.I. Elgerd, E. Fosha, Optimum megawatt-frequency control of multiarea electric energy systems, IEEE Trans. Power Appa. Syst. 89 (4) (1970) 556–563.
[2] N. Cohn, Some aspects of tie-line bias control on interconnected power systems, Am. Inst. Elect. Eng. Trans. 75 (1957) 1415–1436.
[3] J. Kumar, K. Ng, G. Sheble, AGC simulator for price-based operation: part I, IEEE Trans. Power Syst. 12 (2) (1997) 527–532.
[4] H. Bevrani, Intelligent Automatic Generation Control, Springer, New York, 2009.
[5] J. Kumar, K. Ng, G. Sheble, AGC simulator for price-based operation: part II, IEEE Trans. Power Syst. 12 (2) (1997) 527–532.
[6] I.P. Kumar, D.P. Kothari, Recent philosophies of automatic generation control strategies in power systems, IEEE Trans. Power Syst. 20 (1) (2005) 346–357.
[7] L.L. Lai, Power System Restructuring and Deregulation Trading, Performance and Information Technology, John Wiley & Sons, London, 2002.
[8] V. Donde, M.A. Pai, I.A. Hiskens, Simulation and optimization in an AGC system after deregulation, IEEE Trans. Power Syst. 16 (3) (2001) 481–489.
[9] C. Hwang, C.Y. Hsiao, Solution of a non-convex optimization arising in PI/PID control design, Automatica 38 (11) (2002) 1895–1904.

[10] H. Shayeghi, H.A. Shayanfar, O.P. Malik, Robust decentralized neural networks based LFC in a deregulated power system, Electr. Power Syst. Res. 77 (2007) 241–251.
[11] H. Shayeghi, H.A. Shayanfar, A. Jalili, Multi-stage fuzzy PID power system automatic generation controller in deregulated environments, Energy Convers. Manage. 47 (2006) 2829–2845.
[12] W. Tan, H. Zhang, M. Yu, Decentralized load frequency control in deregulated power environments, Electr. Power Energy Syst. 41 (2012) 16–26.
[13] W. Tan, Y. Hao, D. Li, Load frequency control in deregulated environment via active disturbance rejection, Int. J. Electr. Power Energy Syst. 66 (2015) 166–177.
[14] Y. Ding, A. Lisnianski, P. Wang, L. Goel, L.P. Chiang, Dynamic reliability assessment for bilateral contract electricity providers in restructured power systems, Int. J. Electr. Power Energy Syst. 79 (2009) 1424–1430.
[15] P. Bhatt, R. Roy, S.P. Ghoshal, Optimized multi area AGC simulation in restructured power systems, Int. J. Electr. Power Energy Syst. 32 (2010) 311–322.
[16] S. Debbarma, L.C. Saikia, N. Sinha, AGC of a multi-area thermal system under deregulated environment using a non-integer controller, Electr. Power Syst. Res. 95 (2013) 175–183.
[17] K.J. Aström, H. Panagopoulos, T. Hägglund, Design of PI controllers based on nonconvex optimization, Automatica 34 (5) (1998) 585–601.
[18] E. Yesil, M. Guzelkaya, I. Eksin, Self tuning fuzzy PID type load and frequency controller, Energy Convers. Manage. 45 (2004) 377–390.
[19] E. Rakhshani, J. Sadeh, Practical viewpoints on load frequency control problem in a deregulated power system, Energy Convers. Manage. 51 (6) (2010) 1148–1156.
[20] Z.W. Geem, J.H. Kim, G.V. Loganathan, A new heuristic optimization algorithm: harmony search, Simulations 76 (2) (2001) 60–68.
[21] S. Das, A. Mukhopadhyay, A. Roy, A. Abraham, B.K. Panigrahi, Exploratory power of the harmony search algorithm: analysis and improvements for global numerical optimization, IEEE Trans. Power Syst. Man Cybern. 41 (1) (2011) 89–106.
[22] M. Mahdavi, M. Fesanghary, E. Damangir, An improved harmony search algorithm for solving optimization problems, Appl. Math Comput. 188 (2007) 1567–1579.
[23] M.G.H. Omran, M. Mahdavi, Global-best harmony search, Appl. Math Comput. 198 (2008) 643–656.
[24] Q.K. Pan, P.N. Suganthan, M.F. Tasgetiren, J.J. Liang, A self-adaptive global best harmony search algorithm for continuous optimization problems, Appl. Math Comput. 216 (2010) 830–848.
[25] A. Banerjee, V. Mukherjee, S.P. Ghoshal, An opposition-based harmony search algorithm for engineering optimization problems, Ain Shams Eng. J. 5 (1) (2014) 85–101.
[26] A. Banerjee, V. Mukherjee, S.P. Ghoshal, Intelligent controller for load-tracking performance of an autonomous power system, Ain Shams Eng. J. 5 (2014) 1167–1176.
[27] C.K. Shiva, G. Shankar, V. Mukherjee, Automatic generation control of power system using a novel quasi-oppositional harmony search algorithm, Int. J. Electr. Power Energy Syst. 73 (2015) 787–804.
[28] V. Mukherjee, S.P. Ghoshal, Intelligent particle swarm optimized fuzzy PID controller for AVR system, Electr. Power Syst. Res. 77 (2007) 1689–1698.
[29] K. Ogata, Modern Control Engineering, second ed., Prentice Hall International, India, 1995.
[30] A. Demiroren, H.L. Zeynelgil, GA application to optimization of AGC in three-area power system after deregulation, Int. J. Electr. Power Energy Syst. 29 (2007) 230–240.
[31] B. Tyagi, S.C. Srivastava, A decentralized automatic generation control scheme for competitive electricity markets, IEEE Trans. Power Syst. 21 (1) (2006) 312–320.
[32] Z.W. Geem, Recent Advances in Harmony Search, Springer, New York, 2010.
[33] S.K. Saha, R. Kar, D. Mandal, S.P. Ghoshal, Harmony search algorithm for infinite impulse response system identification, Comput. Electr. Eng. 40 (2014) 1265–1285.
[34] B. Shaw, V. Mukherjee, S.P. Ghoshal, Solution of reactive power dispatch of power systems by an opposition-based gravitational search algorithm, Int. J. Electr. Power Energy Syst. 55 (2014) 29–40.
[35] C.K. Shiva, V. Mukherjee, Comparative performance assessment of a novel quasi-oppositional harmony search algorithm and internal model control method for automatic generation control of power systems, Proc. IEE Gener. Transm. Distrib. 9 (11) (2015) 1137–1150.
[36] D.E. Goldberg, Genetic Algorithms in Search, Optimization & Machine Learning, Pearson Education, India, 1998.
[37] A. Banerjee, V. Mukherjee, S.P. Ghoshal, Real coded genetic algorithm and fuzzy logic approach for real-time load-tracking performance of an autonomous power system, Swarm Evolut. Memetic Comput. 1 (1) (2013) 119–131.
[38] V. Mukherjee, S.P. Ghoshal, Particle swarm optimization-genetic algorithm based fuzzy logic controller for dual input power system stabilizers, Inst. Eng. India 88 (2008) 36.
[39] M. Moradi-Dalvand, B. Mohammadi-Ivatloo, A. Najafi, A. Rabiee, Continuous quick group search optimizer for solving non-convex economic dispatch problems, Electr. Power Syst. Res. 93 (2012) 93–105.
[40] S. He, Q.H. Wu, J. Saunders, Group search optimizer: an optimization algorithm inspired by animal searching behavior, IEEE Trans. Evol. Comput. 13 (5) (2009) 973–990.
[41] A. Haghrah, B. Mohammadi-Ivatloo, S. Seyedmonir, Real coded genetic algorithm approach with random transfer vectors-based mutation for short-term hydro-thermal scheduling, IET Gener. Transm. Distrib. 9 (2015) 75–89.